HUGHES RESEARCH LABORATORIES
Malibu, California

a division of hughes aircraft company

RESEARCH AND DEVELOPMENT PROGRAM FOR RADIATION MEASUREMENTS OF RADIOBIOLOGICAL HAZARDS OF MAN IN SPACE

Summary Technical Report
NAS 2-2366

1 August 1966 through 31 July 1967

TABLE OF CONTENTS

LIST OF ILLUSTRATIONS

FOREWORD

The research carried out under contract number NAS 2-2366 with the NASA Ames Research Center has been accomplished in cooperation with the department of Radiology of the University of California at Los Angeles. The program has been under the direction of Dr. Norman A. Baily, Manager, Space Sciences Department of the Hughes Research Laboratories and Professor of Radiology in Residence at the University of California at Los Angeles. Other personnel assigned or contributing to this program were Mr. Jerald W. Hilbert, Mr. Frederick W. Cleary, and Mr. Wesley M. Akutagawa of the Space Sciences Department of the Hughes Research Laboratories, and Dr. Raymond L. Tanner, formerly of the Department of Radiology of the University of California at Los Angeles.

Availability of the cyclotron beams has been made possible through the cooperation of Professor J. Reginald Richardson of the Department of Physics, University of California at Los Angeles, and Mr. Andrew Koehler of the Harvard University Cyclotron Laboratory.

I. INTRODUCTION

This research program was undertaken to develop methods and apply these to the measurement of radiobiologically significant dosimetric quantities to be used for the evaluation of radiation hazards associated with manned space flights and for the evaluation of high energy proton irradiations of cells and whole animals. The effects of radiation depend not only upon absorbed dose, its gross distribution within the biological entity under study, and the absorbed dose rate, but also upon the manner in which energy is deposited on a microscopic scale within the absorbing material. This is evident from the fact that radiations of different linear energy transfer (LET) will produce different biological effects even when the absorbed dose and dose rate are identical. Many studies have attempted to relate relative biological effectiveness (RBE) to the LET distribution of the dose within the biological entity being observed. Pioneering work in this area was done by Rossi and co-workers[1,2] using spherical energy sensors for the determination of LET spectra. However, inherent limitations of the LET concept have been brought out through their work and they have proposed several alternative parameters[3-5] which are more directly pertinent to the study of frequency distributions of the energy deposition in truly microscopic volumes. Further studies by us have shown that for charged particles, additional modifications of these concepts are necessary.

The absorbed dose at a point is defined only when the absorbed energy divided by the mass reaches a constant ratio for successively smaller volume elements containing the point. However, this constant value must obtain for volume elements still large enough to contain a great many individual particle interactions, otherwise significant statistical fluctuations in this quantity will appear. Since energy is imparted to the medium by discrete interactions in or near charged particle tracks it is evident that the absorbed energy density may have large variations on a microscopic scale even when the absorbed dose is quite uniform over macroscopic volumes. A knowledge of these local energy density variations (i.e., the probability that any given biological microvolume has received a given amount of energy) is essential for fundamental studies in radiobiology, since it must be assumed that the energy instrumental in inactivating a cell originates in a volume which is certainly no larger and probably a good deal smaller than the cell.

This research program thus represents an effort to define both the macroscopic and microscopic distribution of dose deposited by high energy protons in tissue with a view toward expanding the basic ideas inherent in Rossi's concepts and, if possible, developing improved concepts and methods while studying fundamental parameters. It is apparent that one meaningful way of expressing these concepts must certainly be the energy deposited per event in a biologically meaningful volume of proper size and shape. It is hoped that a complete understanding

of the relation between microscopic absorbed energy distributions (particularly the very large energy loss tail found to be characteristic of these distributions) and biological effect might lead to a general model of radiation damage which would, for example, allow predictions of proton or other heavy particle induced damage based on the widely studied and documented effects of x-rays on biological systems.

Studies of the center line depth dose distributions for high energy protons are designed to elucidate the distribution of absorbed dose on a macroscopic scale. It is felt that direct measurement of absorbed dose distributions for high energy protons is of considerable importance not only to future related experimentation with tissue-equivalent proportional counters and solid state detectors but for the evaluation of related radiobiological problems as well. During the past year, studies of the center line depth dose distributions have been extended to two additional energies. These beams, both obtained at the new NASA Langley cyclotron, had energies of 300 MeV and 590 MeV. Because of difficulties in extracting beams with satisfactory uniformity characteristics, only limited data were obtained. Center line depth dose data were obtained to depths of approximately 18 cm and 9 cm for the 300 MeV and 590 MeV beams, respectively. Since the observed distributions are consistent with data obtained at other installations at both higher and lower energies, it is not planned at this time to obtain more complete data at these energies.

The second and major aspect of the work during the past year has been concerned with the development and application of methods for determining microscopic dose distributions. Such distributions consist of the energy deposited per event in biologically meaningful volumes. The aim in this phase of the study is to perfect several tissue-equivalent proportional counters with various shaped collecting volumes which may be used to simulate a wide range of tissue volumes, and to determine the microscopic dose distributions in these simulated volumes for various proton fields. In addition to being of primary importance for radiobiological interpretation of radiation damage, such distributions can also be used to evaluate the distributions obtained in small similarly shaped solid state detectors, which may be useful for studies of high energy proton energy deposition spectra occurring in anatomical situations in which the use of proportional counters would be impossible due to their inherently large physical dimensions. In order to obtain meaningful microscopic dose distributions directly using low pressure proportional counters, however, several criteria must be satisfied. Specifically, both the collection efficiency and the gas multiplication must be uniform at all operating pressures and voltages independent of the path taken by particles passing through the chamber volume. As was reported in the last Summary Technical Report, extensive testing showed the initial electrode design for the 2-inch diameter spherical counter to be

deficient, resulting in poor collection efficiency in the outer portions of the chamber volume. A number of new electrode designs have since been examined using the brass test chamber. The final design consists of a 0.003-inch diameter wire stretched completely across a diameter of the spherical volume, with a voltage on the field shaping electrodes which is approximately 36% of the operating voltage on the center electrode. This electrode design has been thoroughly tested using α-particles in the brass test chamber, and in the Shonka tissue-equivalent proportional counter using protons from the UCLA cyclotron.

Uniformity of volume response is an obvious requirement for use of the tissue-equivalent counters with moderately high energy protons, where the entire counter will be exposed. At lower or higher proton energies, however, a different approach must be used, since a monoenergetic parallel beam of protons sees different effective wall thicknesses when impinging upon different portions of the counter, resulting in differential energy losses or cascade production in the counter wall, and thus different energy protons entering the counter's sensitive volume. Several experimental methods have been examined which would allow proper determination of the frequency distribution of the energy deposition along individual pathlengths, and yield the whole counter (microvolume) response by the proper folding together of the individual partial responses. Several preliminary experiments were undertaken to determine the importance of multiple coulomb scatter and the importance of delta rays which produce their ionization in parts of the sensitive volume not along the path of the primary protons, in order to decide on the approach to be taken. Preliminary absorbed energy distributions, for one effective sphere diameter (1.18 microns of tissue), have been determined as a function of depth in Shonka tissue-equivalent plastic, for protons with initial energies of 44 MeV and 125.5 MeV.

A careful study has also been made of the energy loss distributions for essentially monoenergetic protons over a wide range of effective pathlengths. The highly assymetric shapes of the observed energy loss distributions are characteristic of situations in which the mean energy loss over the pathlength considered is comparable to or less than the maximum possible energy transfer in a single collision with an atomic electron, and have been predicted theoretically by Landau[6] and Vavilov.[7] However, the experimental distributions are slightly wider than those predicted by Landau-Vavilov theory even for the largest mean energy loss studied, becoming much wider at very small mean energy losses. It has been determined that this discrepancy disappears if the effect of distant resonance collisions with the atomic electrons, ignored by the Landau-Vavilov theory, is included. This correction was developed by Blunck and Leisegang.[8] A computer program has been developed to unfold the broadening due to electronic noise, statistics of initial ion pair formation, and electron multiplication statistics from the experimental distributions.

II. CENTER LINE DEPTH DOSE STUDIES – HIGH ENERGY PROTONS

Studies of the center line depth dose distributions found in tissue due to protons are designed to elucidate the distribution of absorbed dose on a macroscopic scale. The extrapolation chamber technique and experimental procedure utilized for these measurements were discussed in detail in a previous summary report. In brief, the measurements consist of the absorbed dose as a function of depth in a polystyrene phantom. The absorbed dose is measured with an extrapolation type ionization chamber. Currents were measured using a modified Townsend balance circuit by integrating the charge collected for a fixed time set by the requirement to collect a standard charge on a transmission type ionization chamber. This phase of the study has been extended during the past year to proton energies of approximately 300 MeV and 590 MeV. Both of these beams were obtained at the new NASA Langley cyclotron facilities. Extreme difficulties were encountered at both energies in attempting to obtain a uniformly spread beam, leaving little time to obtain the center line depth dose data and no time at all to examine the scattering characteristics at these energies. However, preliminary data were obtained at each energy by locating the center line in the center of an area which appeared uniform over at least 2-3 inches on the basis of polaroid film exposures. A planned detailed mapping of beam uniformity using a small ion chamber was not possible due to lack of experimental time. The beam transport system requires study and modification before it will be useful for radiobiological purposes. The resulting center line depth dose data obtained with the extrapolation chamber are shown in Fig. 1, (curves C and D), along with the previous data for 630 MeV and 730 MeV protons. It will be seen that these curves are completely consistent with the data previously obtained in this high energy region.

A thorough discussion was included in the last summary technical report of the factors of importance to an accurate conversion of the experimental data into relative absorbed dose as a function of depth in tissue. At that time it was pointed out that one of the major uncertainties in the conversion is the uncertainty, for low energy protons, in W, the average energy required to produce one ion pair in air, and in the relative stopping powers of air, polystyrene and tissue. At that time it was assumed that for protons completely stopped in the phantom material a significant fraction of the charged particle flux at the characteristic dose peak would have energies in this low energy range. However a recent study by Raju[9] of the distribution of particle energies at the position of the Bragg-peak indicates that this is not the case. This study concludes that the model energy of heavy particles at the Bragg-peak position is approximately 10% of the primary beam energy. A study of the energy distribution at the Bragg-peak position for an initially 49 MeV, proton beam shows, for example, a model energy of 4.9 MeV,

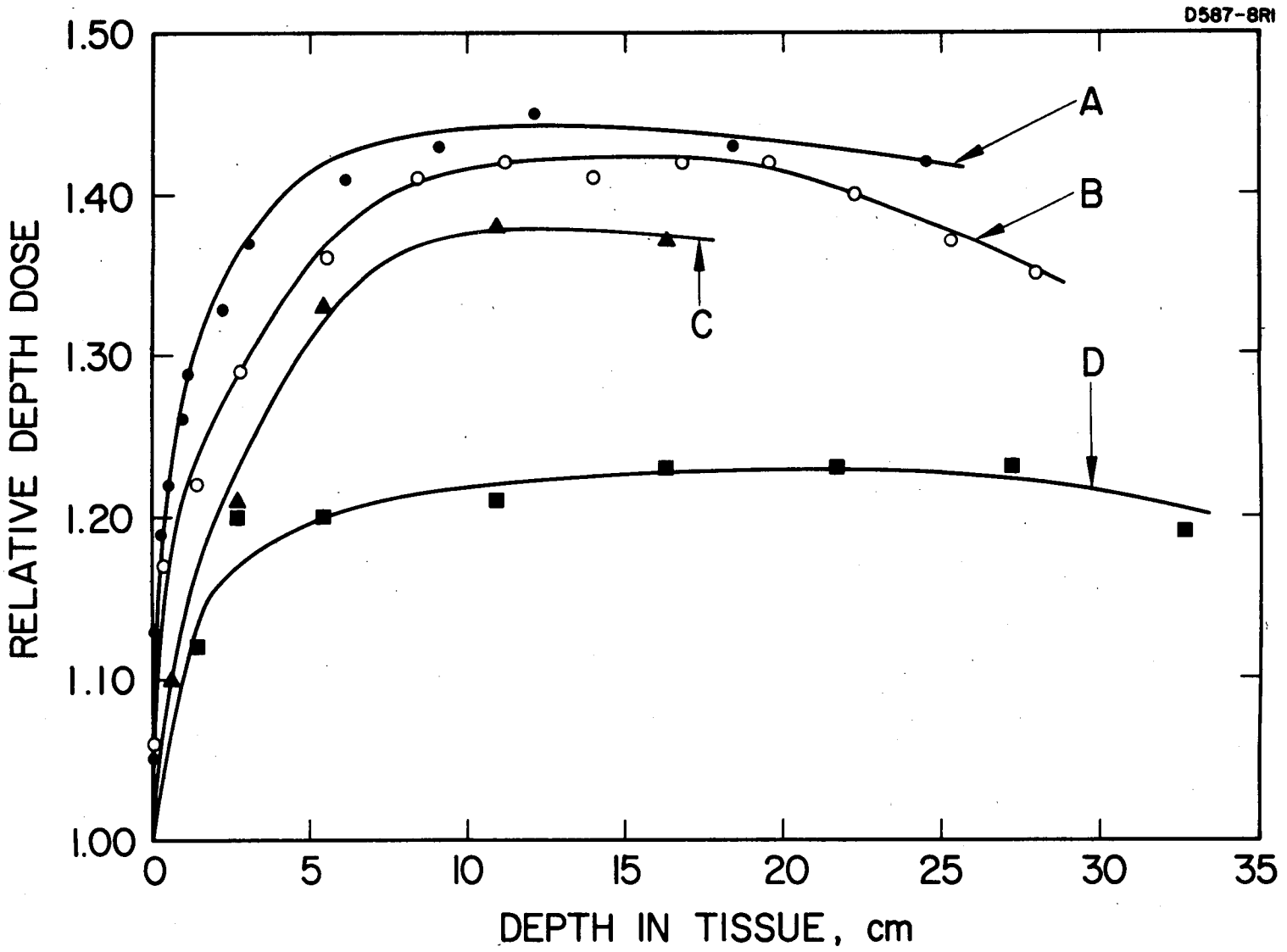

Fig. 1. Center line depth dose curves produced by monoenergetic proton beams incident normally on an infinite phantom. Curves A, B, C, and D represent the data for 730, 630, 590, and 300 MeV, respectively.

with most of the protons having energies between 2 MeV and 8 MeV, over which range the stopping powers and W are fairly well known. Therefore, the uncertainty in these quantities at very low energies does not at all affect the features of the center line depth dose curves of practical importance, namely the position and relative height of the dose peak, making the conversion straightforward. Since the data at 590 MeV and 300 MeV is completely consistent with the data previously obtained at high energies, there are no plans at this time to attempt to obtain more exhaustive data at these energies.

III. MICRODOSIMETRY

A. Counter Design

Microscopic dose distributions depict the variations in the amount of energy deposited per event in biologically meaningful volumes, where the term event refers to the passage through the volume of interest of a single charged particle along with its secondaries. Since enrgy is imparted to tissue by discrete interactions in or near charged particle tracks it is evident that the absorbed energy density may have large variations on a microscopic scale even when the absorbed dose is quite uniform over macroscopic volumes. A knowledge of these local energy deposition variations is essential for an understanding of the biological action of radiation, since it must be assumed that the energy instrumental in inactivating a cell originates in a volume which is certainly no larger and probably a good deal smaller than the cell. The volume most amenable to a simple interpretation is, of course, a sphere, which was originally analyzed by Rossi et al.[1-5] However, there obviously are biological volumes of interest which are more closely approximated by other shapes such as, for example, a cylinder. Bevan[10] has recently suggested parameters analogous to Rossi's Y and Z for a cylindrical volume. The aim in this phase of the study was to simulate tissue volumes of various biologically significant sizes and shapes using tissue-equivalent proportional counters, and to determine the microscopic dose distributions in these simulated tissue volumes for various proton fields. In addition to their importance for radiobiological interpretation of radiation damage, such distributions may be used to evaluate the distributions obtained in very tiny similarly shaped solid state detectors which may be useful for studies of high energy proton energy event distributions occurring in anatomical situations in which the use of proportional counters would be impossible due to their inherently large physical dimensions.

In order to obtain meaningful microscopic dose distributions directly using low pressure proportional counters several obvious criteria must be satisfied. Specifically, both the collection efficiency and the gas multiplication must be uniform at all operating pressures and voltages for ion pairs formed by particles passing through any portion of the chamber volume. Much of the experimental work in the initial phases of this program was concerned with developing a satisfactory electrode design for the 2-inch diameter, spherical, tissue-equivalent proportional counter. The counter is used as a flow counter with a gas filling composed of an equimolar mixture of He and CO_2. The testing methods developed during examination of the initial electrode design of this program and the deficiencies discovered in this design have been discussed in detail in the previous Summary Technical Reports. A number of electrode designs have been examined using the brass test chamber. All of these designs have involved a very small diameter wire stretched completely across the spherical volume. The parameters which

were varied were the wire diameter, the physical structure of the wire supports, including the size and location of the electric field shaping electrodes, and the voltage applied to these field shaping electrodes.

The most optimum design examined consists of a 0.003-in. diameter stainless steel wire stretched completely across the chamber diameter with a potential placed on the field shaping electrodes which is approximately 36% of the collecting potential placed on the center electrode. A very similar design was previously reported to give pulse heights at all test points within 8% of the expected values. However, further testing revealed that this pulse height distribution was not reproducible if the chamber was disassembled and then reassembled between tests. After several attempts to improve the situation by varying the field shaping electrode diameter, it was finally determined that the relatively good pulse height distribution obtained in the one test was an artifact caused by the chance positioning of what turned out to be an unsymmetrical end support. The non-symmetry was caused by the gas inlet and outlet channels, which consisted of a slice along one side of the center insulator and thus exposed more guard ring at this point. The end supports were subsequently redesigned to eliminate this non-symmetry by flowing the gas through two small holes through the center insulator. The distribution of pulse heights obtained in the brass test chamber with this final electrode design, using 1050 volts on the center wire and 382 volts on the field shaping electrodes, is shown in Fig. 2. The values plotted represent the ratios of the experimental to theoretical pulse heights (using the pulse height produced by particles traversing a diameter) for the various pathlengths. The values in parentheses are the resolutions (FWHM) of the alpha peaks. Although points G and E differ from the theoretical values by about 15% and the resolution at point E is poor, it is thought that this pulse height distribution is satisfactory for its planned application since the distribution in the rest of the chamber, representing most of the sensitive volume, is quite good. In addition, it should be pointed out that although the resolution at E is a large percentage increase in the case of the alpha particle test pulse which has an inherent theoretical resolution of the order of 20%, when one is measuring pulses from particles leaving much less energy in the sensor, and hence with much larger inherent resolutions, this degree of counter resolution is not a serious problem.

This electrode design has been incorporated into the 2-inch diameter tissue-equivalent, proportional counter (see Fig. 3) and tested using both 140 keV x-rays and protons from the UCLA cyclotron. The tests performed on the counter using x-rays were designed to ensure that complete collection was attained from all parts of the spherical volume, and also to determine absolute gain figures over a range of normal operating voltages and gas pressures. Complete collection was verified by exposing the whole counter to a constant x-ray intensity and measuring

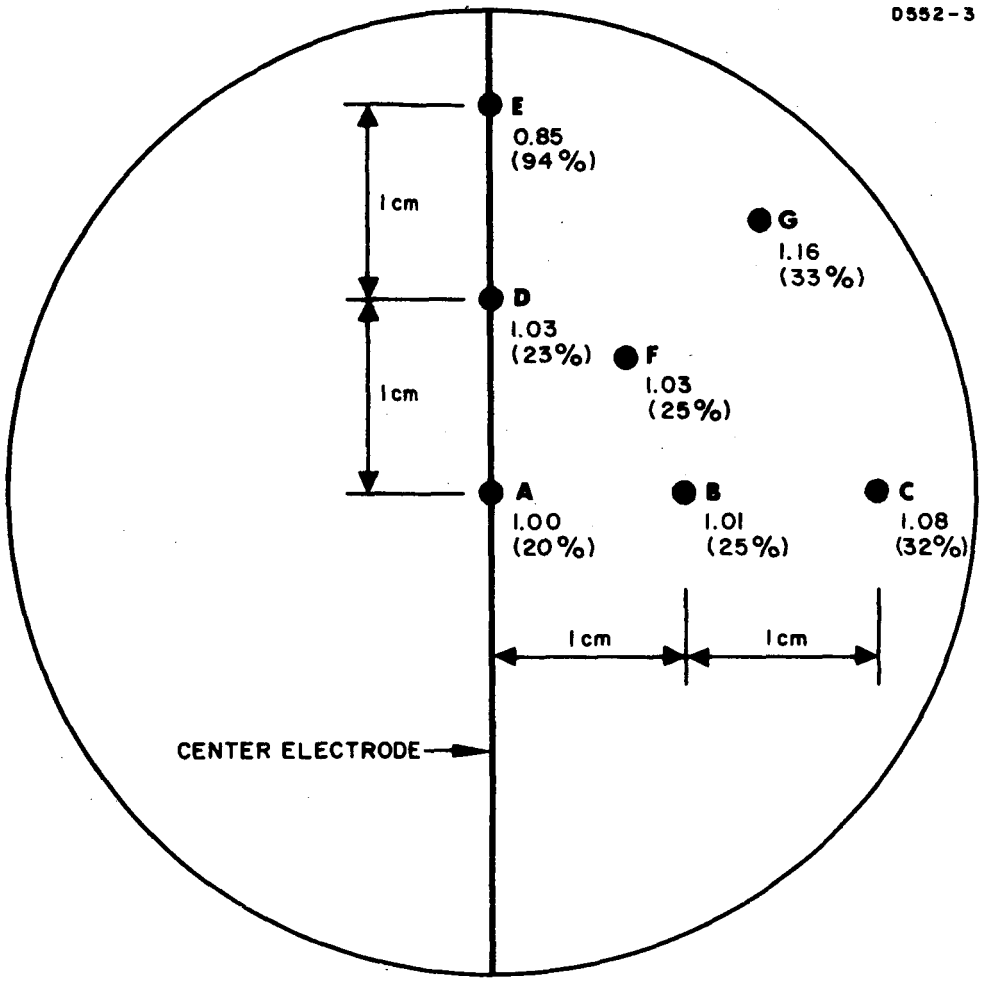

Fig. 2. Volume response of a 2-inch spherical proportional counter having a 0.003-in. diameter center electrode, 20.0 Torr pressure, 1050 V on the center electrode, and 382 V on the field shaping electrodes. Values plotted represent the ratio of experimental to theoretical pulse heights (computed by using the pulse height produced by particles traversing a diameter as the reference signal) for the various alpha particle path lengths. The values in parentheses represent the resolution (FWHM) obtained using Am-241 alpha particles.

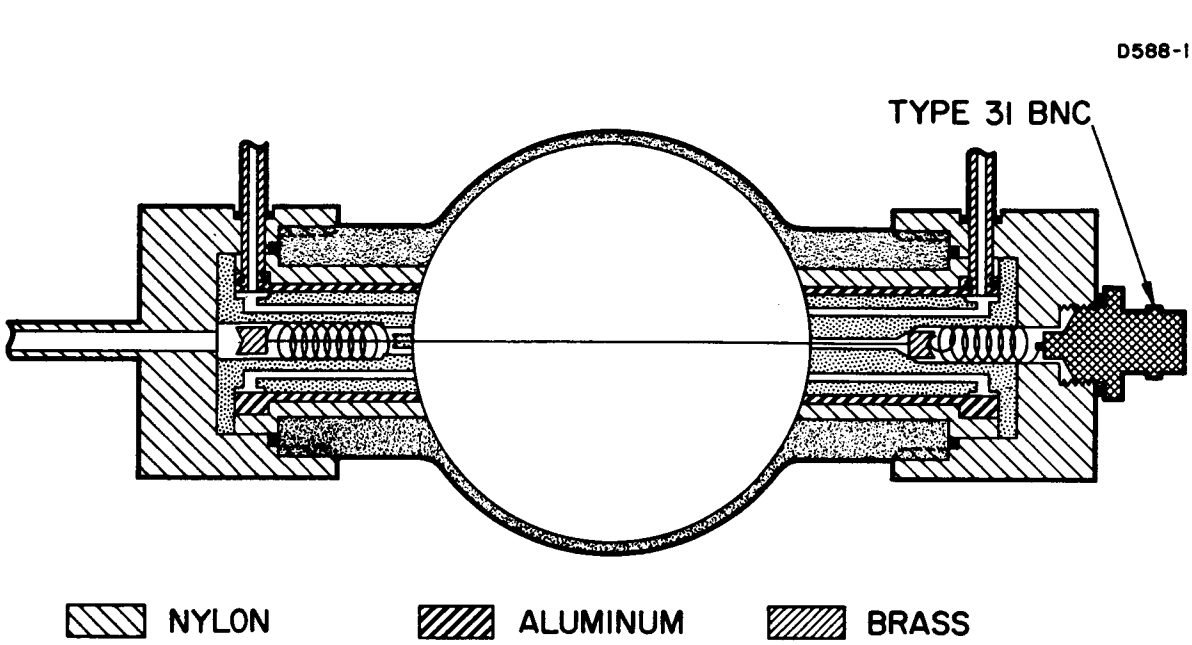

Fig. 3. Electrode design for a 2-inch diameter tissue-equivalent proportional counter.

the current as a function of voltage on the collecting electrode. For the x-ray intensity used, saturation was achieved at about 100 V on the center wire. The absolute gas gain at the center of the counter (with the field shaping electrodes grounded) was measured by collimating an x-ray beam and letting it pass along a diameter of the counter perpendicular to the center electrode. The current obtained as a function of voltage, divided by the saturation current, both normalized to the same x-ray output, is by definition the absolute gas gain at the center of the wire. Representative curves are shown in Fig. 4. The gain was measured only at the center of the wire and with the field shaping electrodes grounded. The relative gain throughout the counter sensitive volume can much more conviently be studied independently for those pressures and operating voltages of interest using alpha particles, and can be converted to absolute gain by reference to any one point on these absolute gain curves. Data of this type are important for correlation of energy deposition spectra taken under different conditions.

The rest of the experimentation performed with the new electrode design in the tissue-equivalent proportional counter has been done using high energy protons. The response of the counter to passage of monoenergetic protons along a single pathlength may be examined by positioning a small frontal area ($\simeq 0.15$ cm^2), silicon, lithium-drifted, p-i-n detector (thick enough to stop a 55 MeV proton) directly behind the proportional counter and operating it in coincidence with the proportional counter. The coincidence circuit uses the output of a variable discriminator level Schmitt trigger to open a prompt coincidence gate in the pulse height analyzer, the Schmitt trigger being actuated by the signals originating in the p-i-n detector. Since the discriminator level in the Schmitt trigger circuit is set to be actuated only by pulses due to peak energy protons, the energy loss distribution obtained from the proportional counter is due only to protons which pass along a well defined straight line path through the counter. The p-i-n detector is also used, of course, to examine the energy characteristics of the proton beams.

The broad, highly assymetric shapes of the energy loss distributions observed in the counter are characteristic of a situation in which the mean energy loss over the pathlength considered is comparable to or less than the maximum possible energy transfer in a single collision with an atomic electron and are adequately described by theoretical treatments, as will be discussed in detail in the next section. However, before a detailed comparison with theory was attempted, a number of experiments were performed to insure that there was no significant distortion of the distributions due to some improper elements in the experimental situation itself. It was initially suspected that scatter and/or proton interactions in the 1/16-inch tissue-equivalent walls of the chamber might tend to distort the distributions. To examine this possibility, the brass test chamber was equipped with very thin

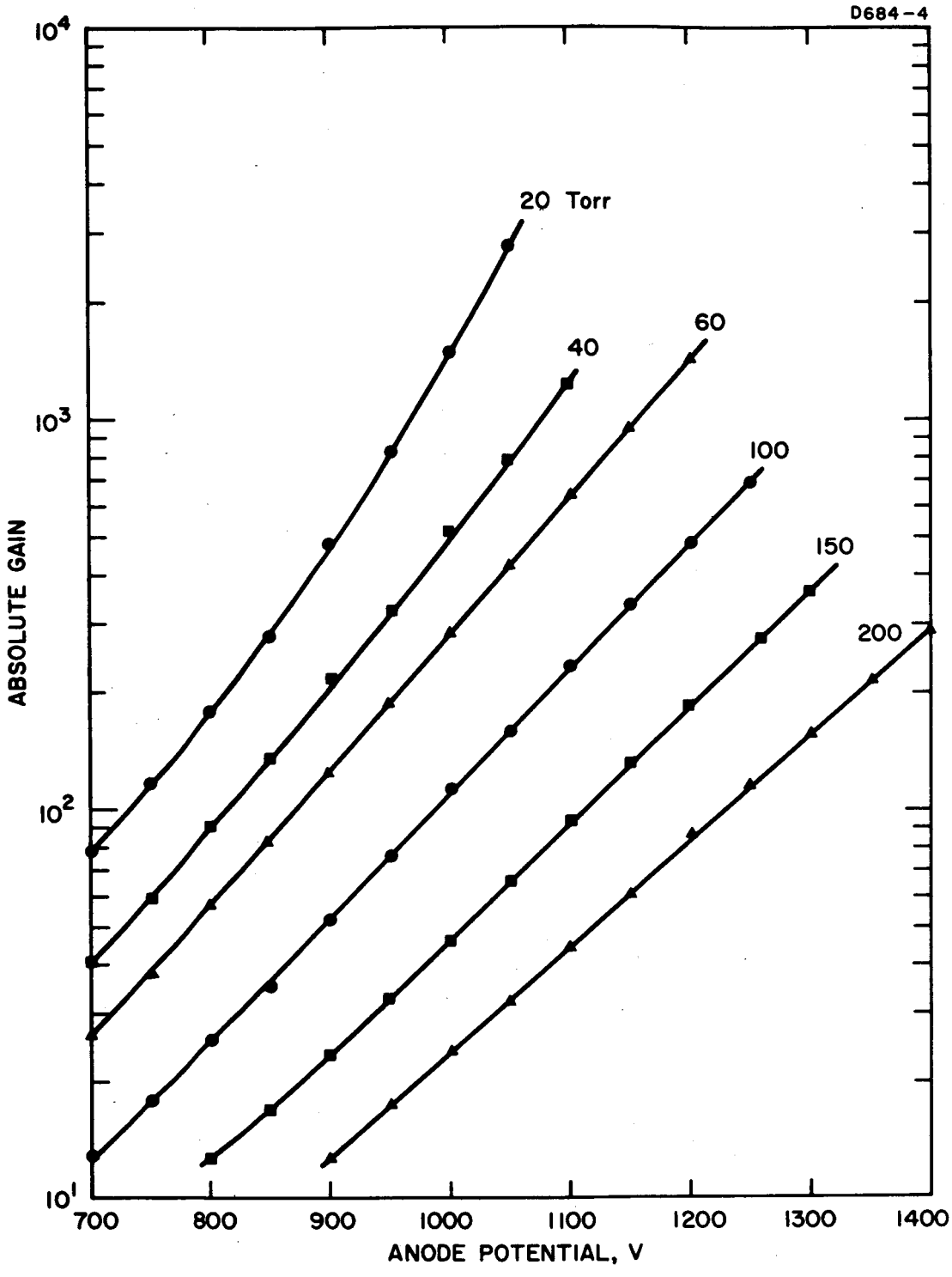

Fig. 4. Absolute gas gain at the center of the spherical, tissue-equivalent proportional counter as a function of applied voltage, for various gas (He-CO_2) pressures.

(0.00025") windows and used in the same coincidence scheme, the effective proton beam passing along a diameter perpendicular to the center electrode, and the resulting energy loss distribution examined under the same conditions. The distribution was essentially the same as that observed through the center of the tissue-equivalent counter. Since the thin windows used in this chamber were observed to bow slightly into the chamber it was determined beforehand that this did not affect the field enough to cause the chamber resolution to deteriorate, by simply passing a collimated alpha beam through one of the thin aluminized mylar windows and observing that the resulting resolution had not changed appreciably from that obtained without a window.

Another possibility examined was that the energy deposition spectrum might be distorted due to pulse pileup and space charge effects. Using a previous electrode design, deterioration of the counter response was observed at high proton fluxes. At that time the coincidence peak was completely obliterated at an average flux of approximately 9000 proton/cm^2/sec. It should be pointed out that this is actually a very high instantaneous counting rate. Since the pulsed beam from the cyclotron is about 3 nanoseconds long with 35 nanoseconds between pulses, the instantaneous proton flux is about ten times the average, or about 90,000 protons/cm^2/sec in this case. In addition, since the whole counter, with an area of about 20 cm^2, was receiving protons, the instantaneous counting rate at which the coincidence spectrum was obliterated was actually 1.8×10^6/sec. In order to determine if the coincidence spectrum was being broadened by this effect, even at the lower counting rates for which the newer coincidence spectra were collected, it was decided to examine the resolution of the peak as a function of counting rate. Variation of the instantaneous count rate by a factor of about 50, from 75,000 counts/sec to 1600 counts/sec, did not change the pulse height distribution by any discernable amount. Since the lower count rate is sufficiently low to preclude the possibility of pulse pileup, this effect cannot be causing any distortion of the distributions.

It will be recalled that previously it had been necessary to position our counter system outside of the main beam and look at the protons scattered at an angle from a thin target. In that situation the intensity of the main energy peak which results from the elastic scatter off of a carbon target, for example, varies quite rapidly with angle. An additional problem is introduced by the presence of lower energy, lower intensity peaks due to inelastic scatter. To overcome these difficulties, a method was worked out with the assistance of cyclotron personnel which resulted in extraction of a spread proton beam of low enough intensity to permit placement of the proportional counter directly in the beam. The examination of resolution as a function of intensity described above was actually done under these conditions. It is interesting to note, and of considerable importance to subsequent experiments, that with our

experiment positioned directly in the main beam it was found possible to effectively collimate the proton beam with a very simple collimator, although this had proved impossible in the previous geometry. Apparently in the previous setup the low intensity scattered protons arriving at our counter were completely overwhelmed by radiation due to interactions of the much more intense main beam with the foil of the vacuum windows, air, etc. The effectiveness of the collimator in this geometry makes it possible to collect pulse height distributions due to essentially monoenergetic protons passing through a fairly well defined path without using the coincidence setup. The comparison of spectra obtained with and without coincidence permits a number of experimental parameters to be examined.

The resolution of the counter itself has been examined using the brass test counter. Under optimum conditions, the resolution (FWHM) of the peak due to Am-241 alpha particles (5.48 MeV) passing across a diameter with a pressure of 20 Torr, has been found to be 16.6% after removal of the noise broadening. The mean energy loss as computed using the tables of Barkas and Berger[11] is 102 keV. Taking into account the broadening due to fluctuations in primary energy loss,[7, 12-14] and the statistical deviations due to variations in primary ionization and electron multiplication, yields a theoretical value of 16.8%. The resolution was also examined by increasing the counter pressure ($\sim$ 600 Torr) until the α-particles were completely stopped in the sensitive volume. After correction for noise broadening, a resolution of 5.7% was obtained. A statistical treatment combined with the experimental results of Campbell and Ledingham[15] shows that the inherent resolution for the experimental conditions used should be 0.5%. The difference between the experimental and theoretical results might be attributed to a number of sources including source thickness, collimation distortion of the energy spectrum entering the chamber, loss of high energy δ rays to the walls, and nonuniformities in the central wire. However, even if the entire difference is due to counter resolution, these results show that the inherent counter resolution, added in quadrature, would distort the broad energy loss distributions of interest insignificantly.

B. Examination of Proton Energy Loss Theory

Numerous tests conducted with the tissue-equivalent proportional counter, using the He-CO_2 (50/50 molar) gas mixture at a pressure of 20 Torr, consistently resulted in very broad energy loss distributions for protons passing along a diameter of the counter. The highly assymetric shape of the energy loss distributions thus obtained (see Fig. 6) is characteristic of a situation in which the mean energy loss over the pathlength considered is comparable to or less than the maximum possible energy transfer in a single collision with an atomic

electron, ϵ_m. However, initial comparison of the experimental results with the widely used Landau[6]-Vavilov[7] theory describing such a situation showed the experimental distributions to be considerably wider than predicted. Further examination of the literature of energy loss distributions, however, has shown that application of a correction to the Landau theory for the effect of distant resonance collisions with the atomic electrons, developed by Blunck and Leisegang,[8] leads to good agreement with the experimental results.

The energy-loss straggling of charged particles traversing a thin layer of matter has been treated theoretically by a number of workers. In 1944, Landau[6] first derived the rigorous equation for the energy-loss distribution function, and solved it analytically in the limit of a very small mean energy loss compared to the maximum possible energy loss per collision. In 1957, P. V. Vavilov published a rigorous solution to the energy loss distribution function without imposing this restriction.[7] The resulting distribution depends on the velocity of the charged particle and on a parameter κ,

$$\kappa = \frac{\xi}{\epsilon_m} \quad ,$$

where

$$\xi = \frac{2\pi e^4 z^2 NZX}{mv^2} \quad ,$$

where $e \equiv$ charge of the electron,

$z \equiv$ particle charge number,

$N \equiv$ number of atoms/cm^3 of the material,

$Z \equiv$ atomic number of the material,

$m \equiv$ electron mass,

$v \equiv$ particle velocity,

and $X \equiv$ pathlength in cm.

Thus κ is indicative of the ratio of the mean energy loss over the pathlength under consideration to the maximum possible energy loss per collision. For $\kappa \gtrsim 0.01$, the Vavilov distribution reduces to the Landau

distribution while for $\kappa \gtrsim 10$ it becomes a Gaussian distribution. Vavilov's distribution, has recently been very conveniently presented in the form of tables by Seltzer and Berger.[16]

In 1950, Blunck and Leisegang[8] considered quantitatively the problem of a correction to the shape of Landau's distribution due to losses to bound electrons, where the amount of energy transferred is of the order of the binding energies of the various atomic shells. They took into account the second moment of the resonance collision spectrum by summing over all bound electrons and their associated ionization energies, and predicted that significant broadening of the energy-loss distribution should occur when their parameter b^2 is greater than three:

$$b^2 = \frac{20\bar{\Delta}Z^{4/3}}{\xi^2} ,$$

where all energies are expressed in electron volts. They also showed that Landau's solution was equivalent to neglecting all moments of the collision spectrum but the first. While this correction was originally applied by Blunck and Leisegang to Landau's solution, as shown by Fano,[17] it may equally well be applied to the solution of Vavilov. Unfortunately, the resulting expression involves a rather difficult and tedious integration to make the correction, and no attempt has been made, to our knowledge, to perform a numerical quadrature of this expression or produce tabulated values, thereby making the corrected theoretical distributions readily available for direct comparison to experiment. We did not consider it worthwhile at this time to write a computer program to make such corrections. As will be shown presently, this correction is of considerable importance for the distributions of interest to us.

Since for the conditions initially examined by us $\kappa \simeq 0.001$, we obviously were in a region in which the "Landau-type" distribution would be expected, but the experimentally determined resolution (FWHM) was of the order of $2\frac{1}{2}$ times that predicted by the theory and extensive testing had indicated that the proportional counter was operating properly and that the experimental parameters were such that it should have been correctly measuring the desired energy loss distribution. While at this time we were not aware that the Blunck-Leisegang theoretical treatment would properly predict the energy loss spectrum for a situation in which the mean energy loss is so small that losses to bound electrons significantly affect the resulting distribution, it was obvious that we were operating in a region in which one of the conditions for applicability of the Landau-Vavilov formulations was violated. Both of

these formulations require that $\xi/\epsilon_o \gg 1$, where ϵ_o is a characteristic energy of the order of the mean electron binding energy. For our gas mixture $\epsilon_o \cong 13.5$ eV, computed as recommended in NBS Handbook 79.[18] Therefore $\xi/\epsilon_o \simeq 9$ and this condition is not met. Therefore the simple Landau-Vavilov theory is not applicable. In order to insure, therefore, that the proportional counter was, in fact, correctly measuring the energy loss distribution, it was decided to examine the counter response over a range of pressures in which all the conditions are met for the validity of the Landau-Vavilov treatments. This resulted in a series of energy loss distributions which, it turns out, serve as a very nice check on the Blunck-Leisegang correction for this very small mean energy loss region in which no experimental verification has previously been performed. In addition, it was possible to obtain a sufficiently thick pathlength to reach a region which had been experimentally verified using a proportional counter to measure the energy loss of protons with energies comparable to those available to us. These distributions were obtained using both the Shonka tissue-equivalent proportional counter and, as a double-check, using the brass test counter with thin (0.00025" mylar) entrance and exit windows.

Figure 5 shows the distribution obtained with 43.7 MeV protons passing through a gas path of 4.00 mg/cm^2 (600 Torr pressure in the brass test counter) compared to that predicted by Vavilov. This distribution represents the largest mean energy loss (49.5 keV) examined, and therefore requires the smallest Blunck-Leisegang correction factor. Energy loss distributions for mean energy losses ranging down to 1.64 keV are shown in figs. 6 through 10. The experimental conditions for all of these distributions are summarized in table I and the experimental results in table II.

The energy loss distribution at 600 Torr is in a region comparable to that examined experimentally by Gooding and Eisberg[19] using an argon filled proportional counter to study the energy loss distributions of 37 MeV protons. Their broadest energy loss distribution had a mean energy loss, $\overline{\Delta}$, of 34 keV and a κ of 0.0425 compared to $\overline{\Delta}$ = 49.5 keV and κ = 0.0375 for our data shown in Fig. 5. The agreement of the experimental resolution (FWHM) obtained for our situation with the Vavilov theoretical resolution (42% experimental versus 37% theoretical) is comparable to that obtained by Gooding and Eisberg (50% experimental versus 45% theoretical), the experimental resolution being consistently somewhat greater than predicted by Vavilov's formulation even for κ values in this range (Gooding and Eisberg actually compared their results to a theory developed by Symon[13,14] for intermediate κ values, but Seltzer and Berger[16] have shown that Symon's theory leads to essentially the identical result as Vavilov's). It will be noted that as the mean energy loss decreases and the Blunck-Leisegang parameter b^2 increases, the correction to the Vavilov theory becomes

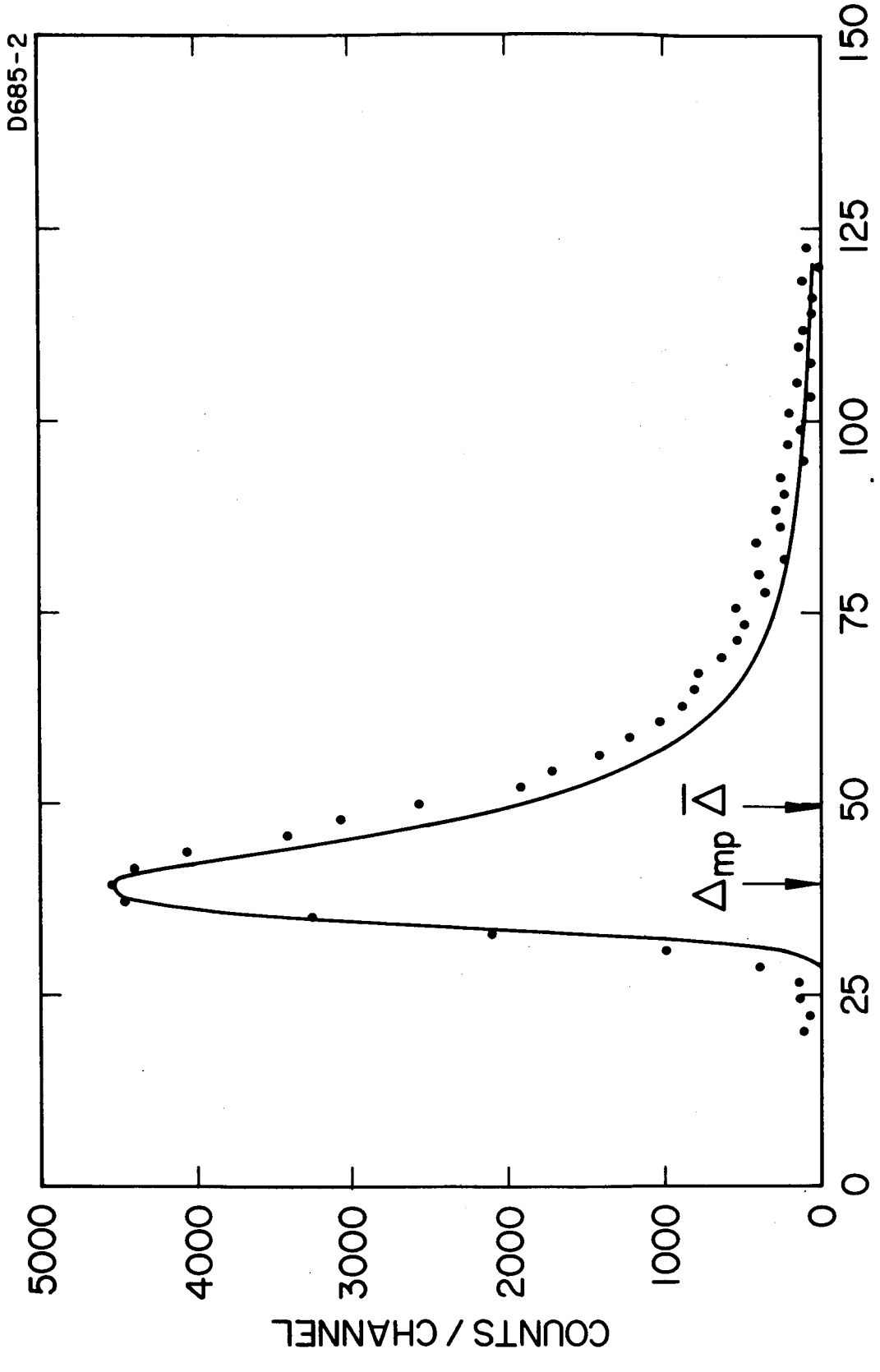

Fig. 5. Comparison of the Vavilov theoretical energy loss distribution (full curve) with an experimentally observed distribution (plotted points) for 43.7 MeV protons passing through 4.00 x 10^{-3} g/cm^2 of a He-CO_2 (50/50 molar) gas mixture.

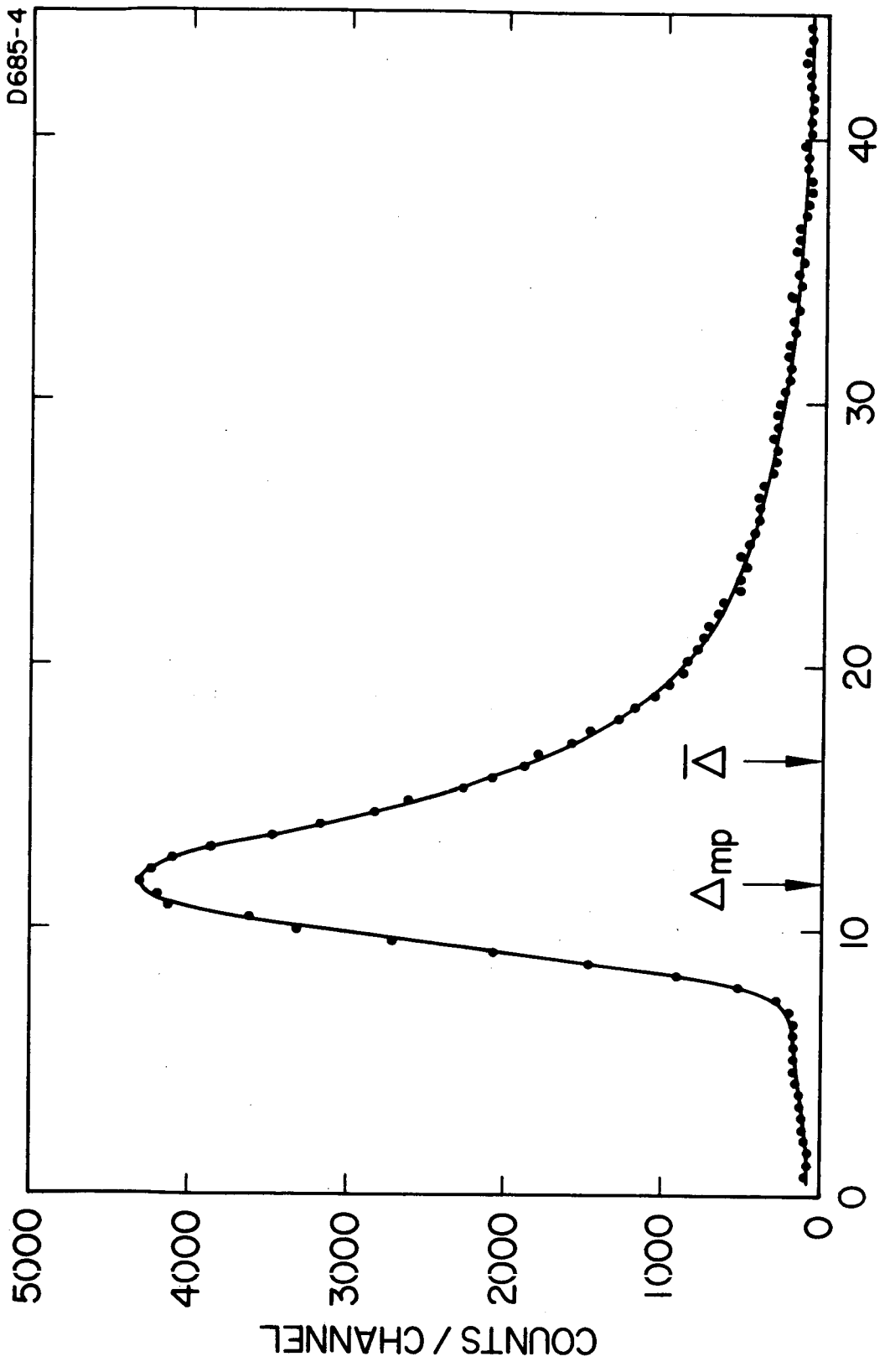

Fig. 6. Frequency distribution for the energy deposition of 43.7 MeV protons passing through 1.33×10^{-3} g/cm^2 of a He-CO_2 (50/50 molar) gas mixture.

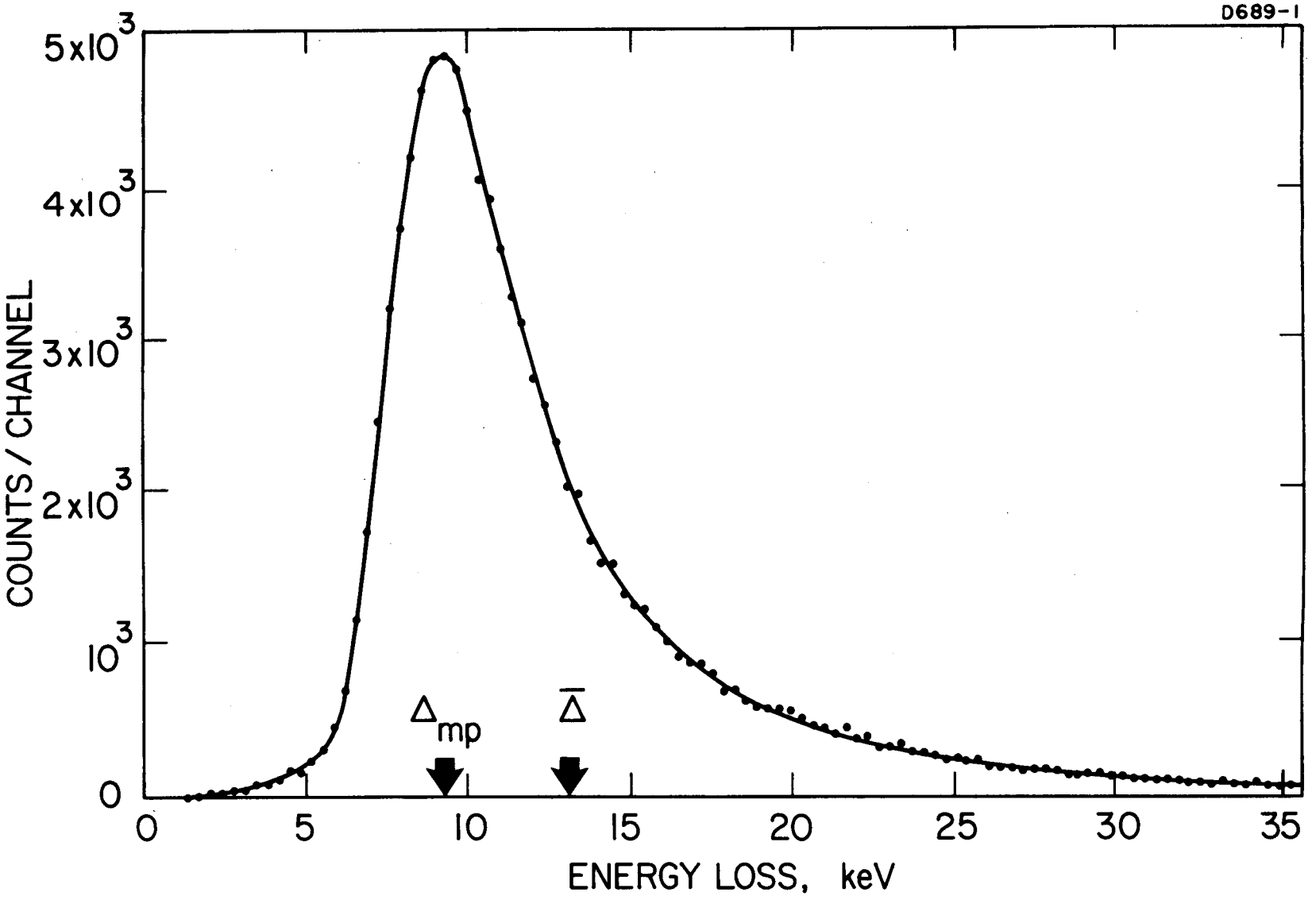

Fig. 7. Frequency distribution for the energy deposition of 40.3 MeV protons passing through 1.00×10^{-3} g/cm^2 of a He-CO_2 (50/50 molar) gas mixture.

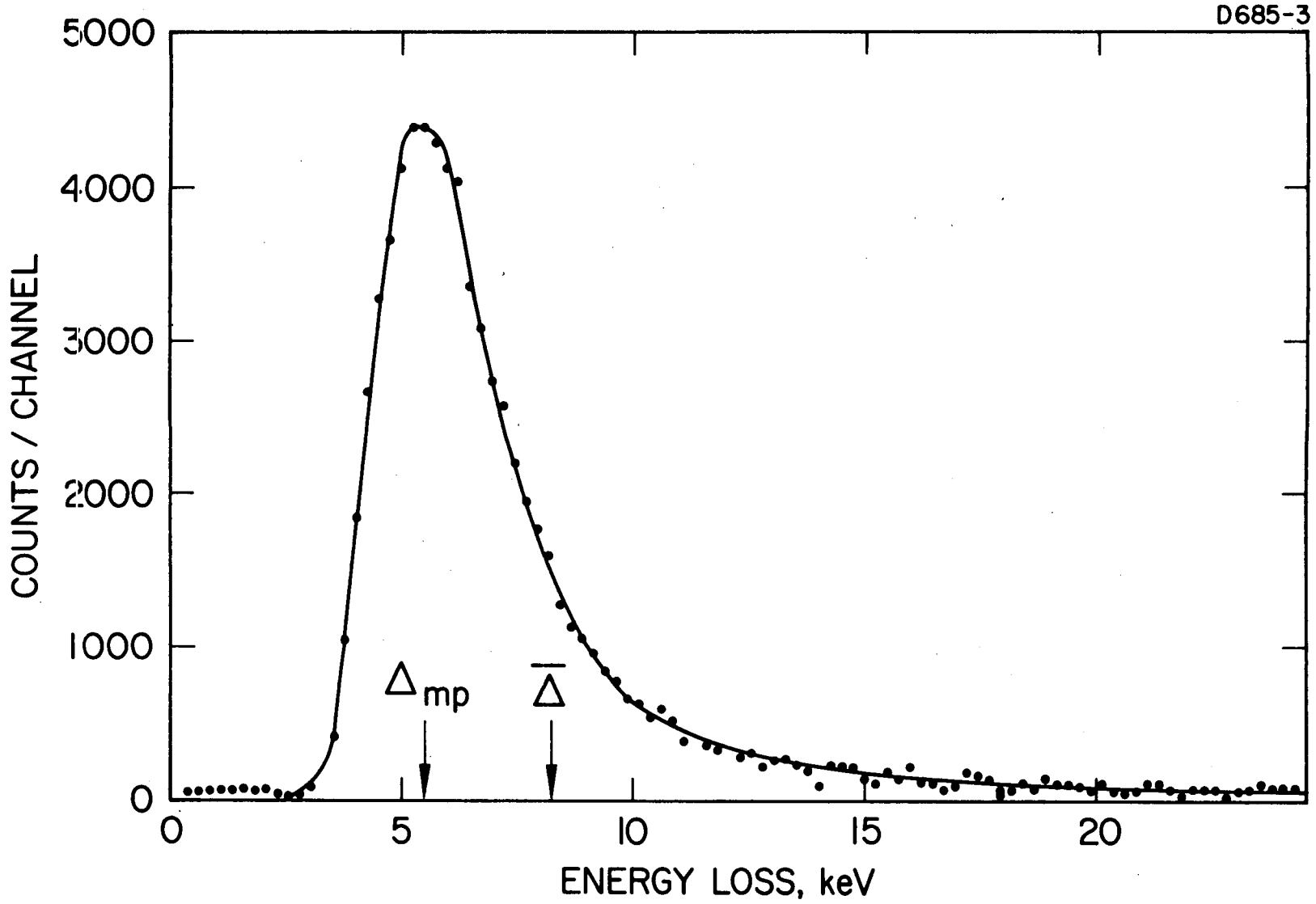

Fig. 8. Frequency distribution for the energy deposition of 43.7 MeV protons passing through 6.66×10^{-4} g/cm^2 of a He-CO_2 (50/50 molar) gas mixture.

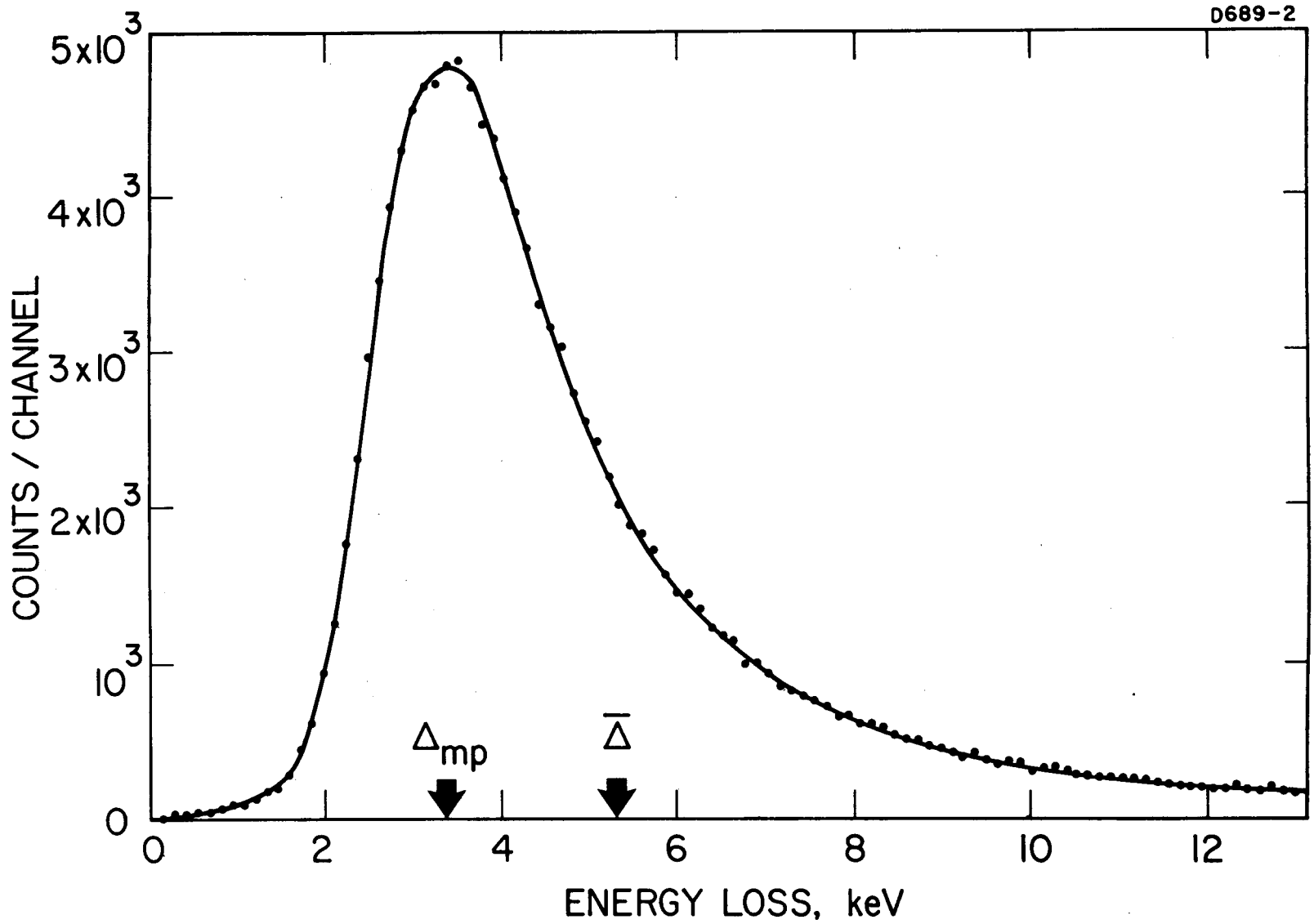

Fig. 9. Frequency distribution for the energy deposition of 40.3 MeV protons passing through 4.00 x 10^{-4} g/cm^2 of a He-CO_2 (50/50 molar) gas mixture.

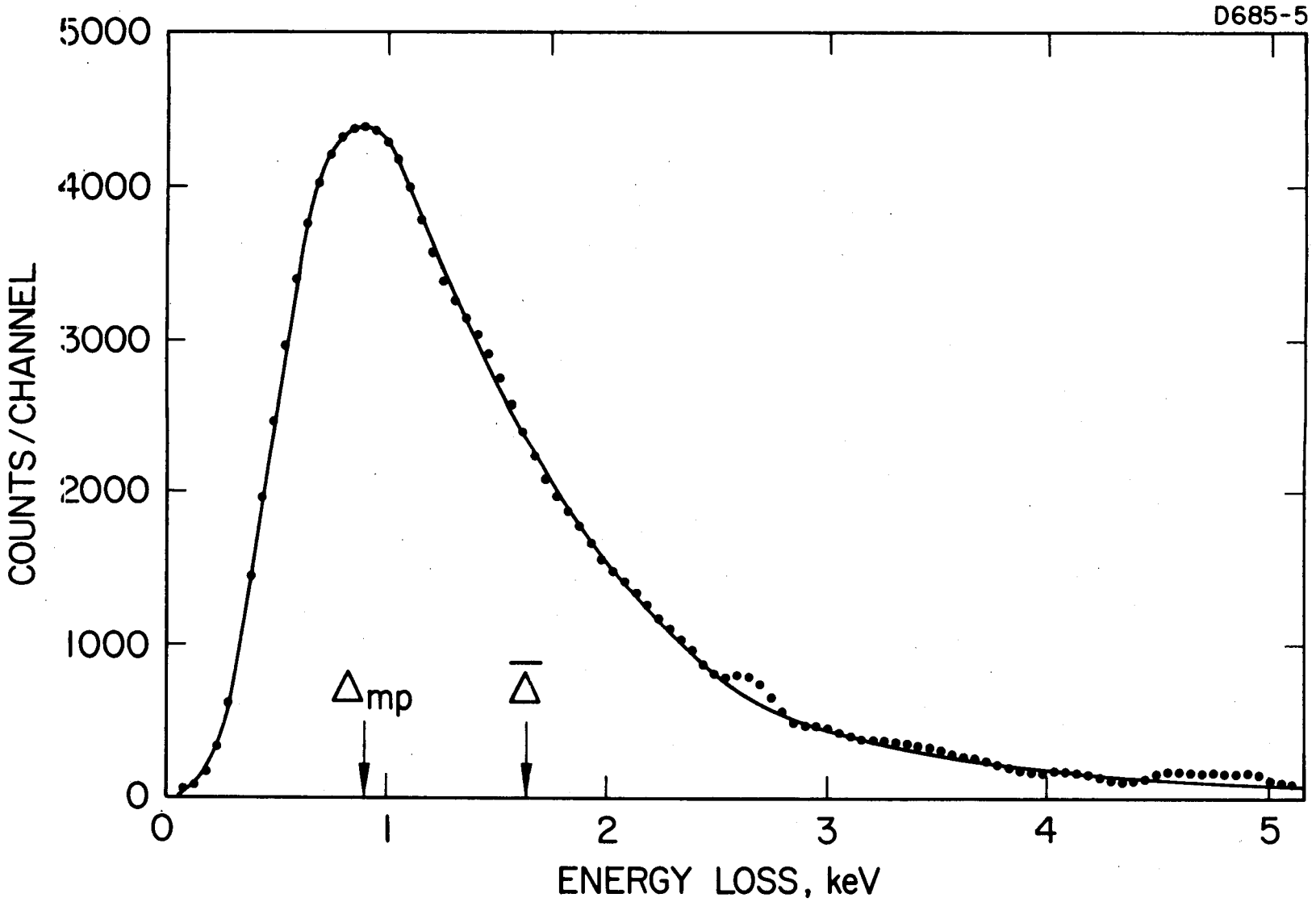

Fig. 10. Frequency distribution for the energy deposition of 43.7 MeV protons passing through 1.33×10^{-4} g/cm^2 of a He-CO_2 (50/50 molar) gas mixture.

more and more important. The Blunck-Leisegang corrected theoretical resolutions listed in table II have associated with them an uncertainty of approximately ± 2%, due to the accuracy with which the correction factor can be read from published curves.[20] As a result of the counting statistics associated with each of the individual experimental points the reported resolution values have an uncertainty of approximately ± 3%, estimated graphically from the extremes of the smooth curves which could be drawn through the points. In all cases examined the agreement between the experimental results and the theoretical predictions using the Blunck-Leisegang correction is very good.

The experimental resolutions reported for the brass counter have been corrected for noise broadening and for the broadening due to statistical fluctuations in the number of initial ion pairs formed in the gas per unit of energy deposited and the fluctuations in the number of avalanche electrons created per primary electron-ion pair formed in the gas. This was done by writing an iterative computer program to apply the correction method originally described by Freedman, et al.[21] The noise broadening was assumed to produce a gaussian spread in pulse heights. The corrections for the statistics of ion pair formation and multiplication were made using the Poisson type of distribution originally worked out by Snyder[22] and others, and most recently studied experimentally by Campbell and Ledingham.[15] The average energy required to produce an ion pair in the gas mixture was computed using the method of Bortner and Hurst,[23] and using values of 31.5 eV for contaminated helium and 33.5 eV for CO_2. This yields a value of 31.7 eV for the mixture. These corrections resulted in a maximum change in resolution of 3% for the distributions examined. Since these corrections were so small, the data obtained in the Shonka counter were not corrected in this manner. It should be noted that the periodic structure seen in the tails of the computer corrected curves is an artifact introduced by the computer program.

Several additional comments should be made concerning tables I and II. The average energy loss, $\overline{\Delta}$, was computed using Barkas and Berger's[11] two-variable stopping power tables, using effective values for Z/A and the mean excitation potential, I, computed according to[18]

$$\frac{Z}{A} = \sum_i \mu_i \frac{Z_i}{A_i} \quad ,$$

and

$$\ln I = \left(\frac{Z}{A}\right)^{-1} \sum_i \mu_i \frac{Z_i}{A_i} \ln I_i \quad ,$$

where μ_i is the fraction by weight of the $i^{\underline{th}}$ compound in the mixture. The relative skewness of the various distributions is indicated by the ratio of the most probable energy loss (peak of the distribution) to the mean energy loss, $\overline{\Delta}mp/\overline{\Delta}$. The ratios listed in the table are computed from theory, but an integration of the experimental curves (using a planimeter) for 600 Torr and 200 Torr gave excellent agreement with the theoretical ratio. The theoretical resolution associated with a Vavilov distribution corresponding to the 600 Torr experiment was measured from the plotted theoretical distribution, while for all other pressures it was computed according to the relation,

$$FWHM_{Landau} = 3.98\ \xi \quad ,$$

which has been shown by Breuer[24] to hold for Landau distributions. It might be noted that the product $\overline{\Delta} \times \overline{A} \cong 5 \times 10^6$ eV for all cases, which is well below the "good behavior criterion" limit reported by Hanna, Kirkwood, and Pontecorvo,[25] and since verified by a number of experiments. This criterion requires that this product be less than 10^8 eV.

One additional very important point should be kept in mind when comparing experimental distributions with any of these theoretical treatments. The Landau-Vavilov theory, with or without Blunck-Leisegang corrections, predicts the distribution of energy <u>losses</u> by the protons on passing through the sensitive volume of the proportional counter while the spherical proportional counter obviously measures only the energy <u>absorbed</u> in the sensitive volume. These two quantities will only be equal if the pathlength available to secondaries in the detector is greater than the range of the maximum energy delta rays which may be produced. If a significant number of delta rays should deposit only part of their energy in the counter, this could change the absorbed energy spectrum considerably. The magnitude of this effect and its exact influence on the resulting distributions is very difficult to predict accurately. However, we can get an estimate of the importance of these effects by calculating the fraction of the total energy loss in the counter

given on the average to electrons whose range is comparable to or greater than our detector thickness:

$$\frac{\bar{\Delta}(\delta \text{ ray})}{\bar{\Delta}(\text{total})} = \frac{\ln\left(\epsilon_{max}/\epsilon_{\delta}\right)}{\ln\left(\epsilon_{max}/\epsilon_{min}\right)} = \frac{\ln\left(\epsilon_{max}/\epsilon_{\delta}\right)}{2\ln\left(\frac{\epsilon_{max}}{I}\right)} \quad .$$

This ratio, for 40 MeV protons, is approximately 5%, 8% and 11% for pressures of 600, 200 and 100 Torr, respectively. It is very difficult to estimate this quantity accurately for the case of 20 Torr pressure since the thickness of the counter ($\simeq 10^{-4}$ g/cm^2) is below the range covered by available range-energy tables for electrons. An extrapolation beyond the range covered gives a very crude estimate of 20% for the ratio in this case. Thus, this effect may be of some importance for proton energies in this range for the range of tissue volumes simulated. However, for small κ such as obtain for all of our distributions, this effect will only distort the tail of the distribution and not affect the width of the peak, since the peak is primarily due to the numerous low energy delta rays. Comparison of the resolutions (% FWHM) is therefore still a very meaningful measure of the agreement between theory and experiment. In addition, it should be strongly emphasized that to the extent that this effect may be of importance it represents a limitation only in the sense of complicating the comparison of the complete experimentally determined energy absorption distributions with the theories predicting the energy loss distributions of charged particles, since exactly the same thing would occur in a microsphere of tissue and the resulting experimental energy absorption distribution would be exactly that which is of importance biologically. This is one of the important reasons for determining such energy deposition distributions directly even in simple cases.

It might be noted that while most previous experimental studies of "Landau-type" distributions have been carried out with electrons, a number of experimenters have obtained distributions broader than predicted by the Landau-Vavilov theory. In a series of experiments by Rothwell,[26] West,[27] and Bradley,[28] for example, using a proportional counter filled with either neon, argon, or krypton to measure the energy loss distributions due to minimum ionizing electrons, it was found that the most probable energy loss was correctly given by the Landau theory but that the experimental distributions were considerably wider than predicted. Kageyama, et al[29] found good agreement with the Blunck-Leisegang theory for passage of conversion electrons through thin metal foils.

C. Frequency Distributions of Microscopic Energy Deposition

Since extensive testing has now shown that the proportional counters and the coincidence scheme performs properly within the limits of the pertinent parameters, determination of microscopic energy deposition distributions has been initiated. This is accomplished in this relatively low energy range by exploring the counter response with small diameter beams. The variation in effective wall thickness across the area of the counter is sufficient to change the energy of protons entering the sensitive volume significantly and therefore, if one were to attempt to imbed the counter in a phantom for protons in this energy range, the results would be completely meaningless. For 46 MeV protons, for example, with the counter as close to the surface of the phantom as is possible, 13% of the counter would be at a depth greater than the range of the protons. The situation is quite different, of course, at higher energies or with smaller counters. Therefore, while this chamber can be used at higher energies, in this energy range the energy deposition spectra must be determined by observing the spectrum due to protons passing along a diameter, and utilizing changes in gas pressure to change the effective pathlength in the simulated tissue microvolume. Before describing results of this type of examination, however, several related experimental results should be examined which were instrumental in crystallizing the experimental approach taken.

Our first test was performed to determine the importance to the energy deposition spectra of delta rays which produce their ionization in parts of the sensitive volume not along the path of the primary protons, and thus to determine the importance of the shape of the sensitive volume used to examine energy deposition distributions along individual pathlengths. Since the gas gain along the center electrode is quite uniform with the proper voltage applied to the field shaping electrodes but very nonuniform when they are grounded, coincidence spectra for protons passing along a diameter perpendicular to the center electrode would be expected to differ for the two situations if there is a significant contribution to the energy deposition spectra from delta rays which produce their ionization in portions of the sensitive volume other than essentially along the primary proton path. This was examined at 20 Torr, since the effect would be most pronounced at low gas pressure, for two reasons. First, a given energy delta ray ejected at an angle to the proton path would travel further into other parts of the sensitive volume. Second, the nonuniformity of gain along the wire increases with a decrease in gas pressure, making the test more sensitive. No change in the shape of the distribution due to this cause was observed either for coincidence or collimated only spectra. However the sensitivity of such a test is hard to evaluate. Assuming that multiple coulomb scatter is small, so that the energy spectrum for a small beam at a given depth is essentially the same as would occur at the same depth for

an infinitely broad beam, the energy deposition spectrum may be determined at a given tissue depth by observing the spectrum along a fixed path while changing the gas pressure to change the effective pathlength in the simulated tissue microvolume. The response of an entire spherical, or arbitrarily shaped, microvolume at that depth can then be obtained by folding together the distributions on the basis of the relative number of pathlengths of each value in the given geometrical shape.

While it is well established[17, 30] that multiple coulomb scattering, represented as the average difference between the depth of penetration and the total pathlength of protons, is of the order of only a few tenths of one percent for protons in this energy range stopping in low Z materials, experiments have been performed to investigate directly whether multiple coulomb scatter may be ignored in our experiments. It was previously observed that spectra taken with a collimated proton beam were consistently somewhat broader than those taken in the coincidence mode. This was initially interpreted as most probably due either to small angle scattering in the tissue-equivalent walls or due to poor collimator alignment. Several results now point to collimator effects as the most probable cause, indicating that multiple scattering in the walls is probably of much less importance than was first suspected. The first evidence was a direct test of this point, in which a collimated beam was observed in the brass test counter, first through only the thin entrance window and then through a 1/16-inch piece of tissue-equivalent plastic directly in front of the window. Since no difference was observed, multiple scattering, at least after passage of the protons through this thickness, cannot be a significant factor. Second, using an improved collimator design, during one run the difference between collimated and coincidence spectra was found to be insignificant. This was interpreted as due to fortuitous good alignment, thus eliminating collimator edge effects, for this particular setup thus again pointing to collimator effects rather than multiple scatter in the walls as causing the difference previously reported between collimated and coincidence spectra. Finally, and most significantly, in the course of the run in which this agreement was observed, coincidence and collimated only spectra were compared with $\simeq 1.22\ g/cm^2$ of polystyrene degrader in front of the counter and no difference was observed. This is very good direct evidence that multiple coulomb scatter is of little importance even at this depth, which is well up on the rising portion of the "Bragg type" curve for this energy proton (40.3 MeV). It will be of interest to perform an anticoincidence experiment to determine whether there is any indication of any contribution at all from multiply scattered protons. This type of experiment should lead to a positive conclusion. The points discussed are pertinent only for this initial energy proton. The situation would be expected to be quite different at higher energies.

All indications are, then, that we can proceed according to the method described above. Accordingly, a preliminary run was made to determine the absorbed energy distributions for one effective sphere diameter (1.18 microns of tissue) as a function of depth in Shonka tissue-equivalent plastic, for protons with an initial energy of 44 MeV. The results of this examination are summarized in table 3. For each depth examined the p-i-n proton spectrum was, of course, that after passage through the second 1/16-inch tissue-equivalent wall and a small air path, rather than the actual energy spectrum entering the simulated microvolume. The energies listed in table 3 are, however, calculated[11] values of the actual mean energies entering the simulated microsphere. It will be noted that the energy deposition distributions retain their characteristic peaked shape even at the largest depths (the last two distributions were obtained with collimated beams only since the residual proton energy was insufficient to reach the p-i-n detector). It should be pointed out that the relative peak heights (representing the most probable energy loss) are not simply related to the relative average stopping power of the protons entering the microvolume, since the ratio $\Delta mp/\overline{\Delta}$ is increasing significantly as the mean energy of the proton spectrum decreases. The widths of the distributions, of course, are determined by the combination of two effects; the fractional width tends to decrease as the mean energy of the incoming protons decreases (increasing the mean energy loss in the cavity), while the increasing energy spread of the proton spectrum tends to broaden the peak of the distribution. Such an interplay would be extremely difficult to predict theoretically with any confidence and points out once again the need for direct measurements of such distributions. Representative proton spectra are seen in Figs. 11 and 12, which are the spectra observed after passing through 0.447 g/cm^2 (first case in table 3) and after 1.59 g/cm^2 (fifth case in table 3), respectively. It will be seen that the FWHM has increased from approximately 3% (1.1 MeV) to approximately 56% (4.4 MeV). The corresponding coincidence spectra are seen in Figs. 13 and 14. It will be noted that the increased energy loss at this depth more than compensates for the large increase in proton energy spread, the combined effect resulting in a distribution with a narrower peak than near the surface.

A similar preliminary run was made using the higher energy protons available at the Harvard cyclotron. An energy calibration performed by the Harvard cyclotron personnel using range in aluminum as the criterion, indicated an initial proton energy of 125.5 ± 0.8 MeV. As a check, a "Bragg type" ionization curve was measured just prior to our experiment. This value is consistent, within the limits of error, with energy measurements made by us using the silicon p-i-n detector. The beam spot had a diameter of $\simeq$ 7mm. Non coincidence spectra for this beam passing along a diameter were collected for depths ranging from the equivalent of 0.21 g/cm^2 of water (one tissue-equivalent wall) to 11.61 g/cm^2 of water (beyond the mean proton range). Coincidence spectra were also obtained for several of the shallower depths.

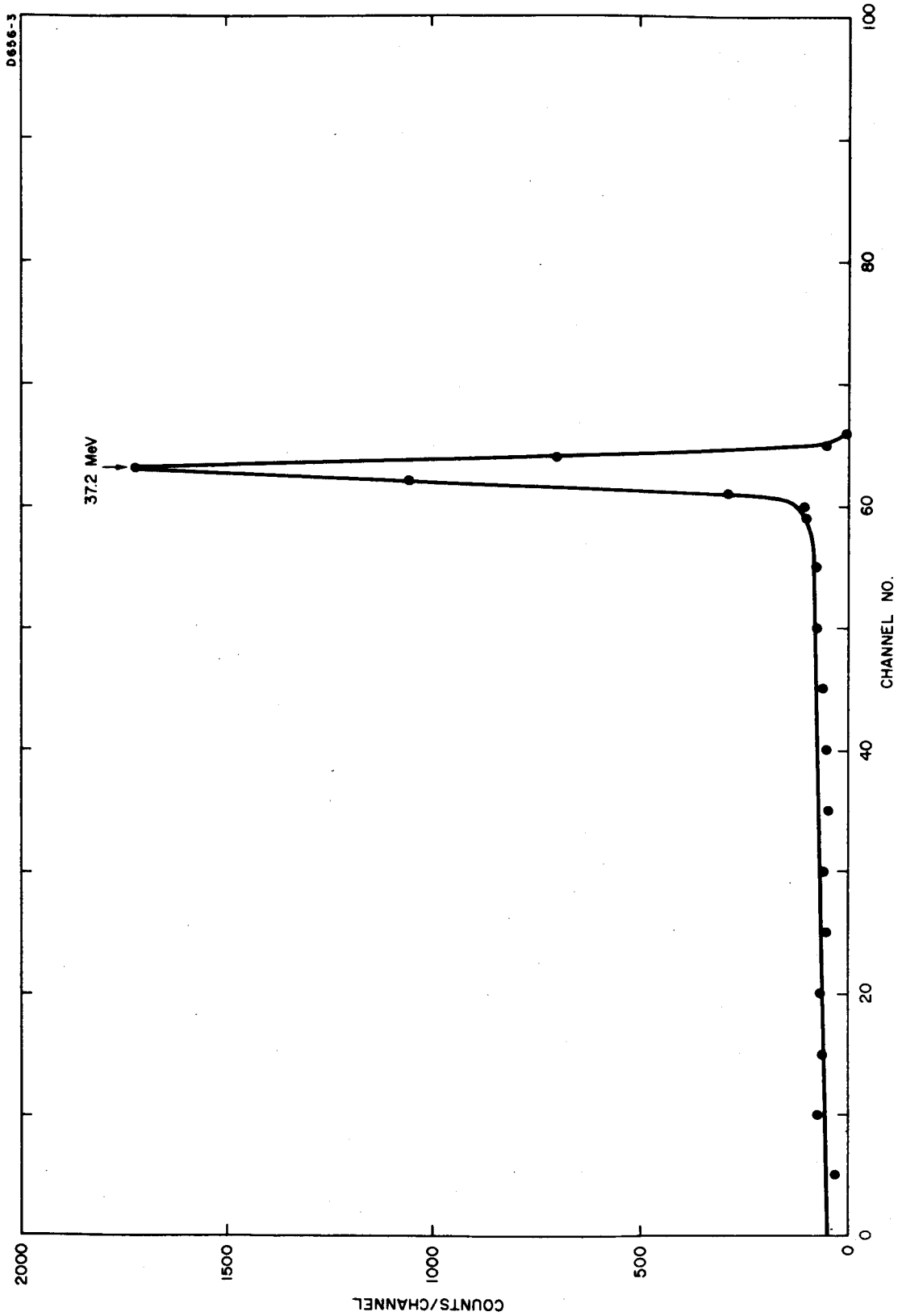

Fig. 11. Energy spectrum of 44 MeV monoenergetic protons after passage through $\cong 0.45$ g/cm^2 of tissue-equivalent plastic.

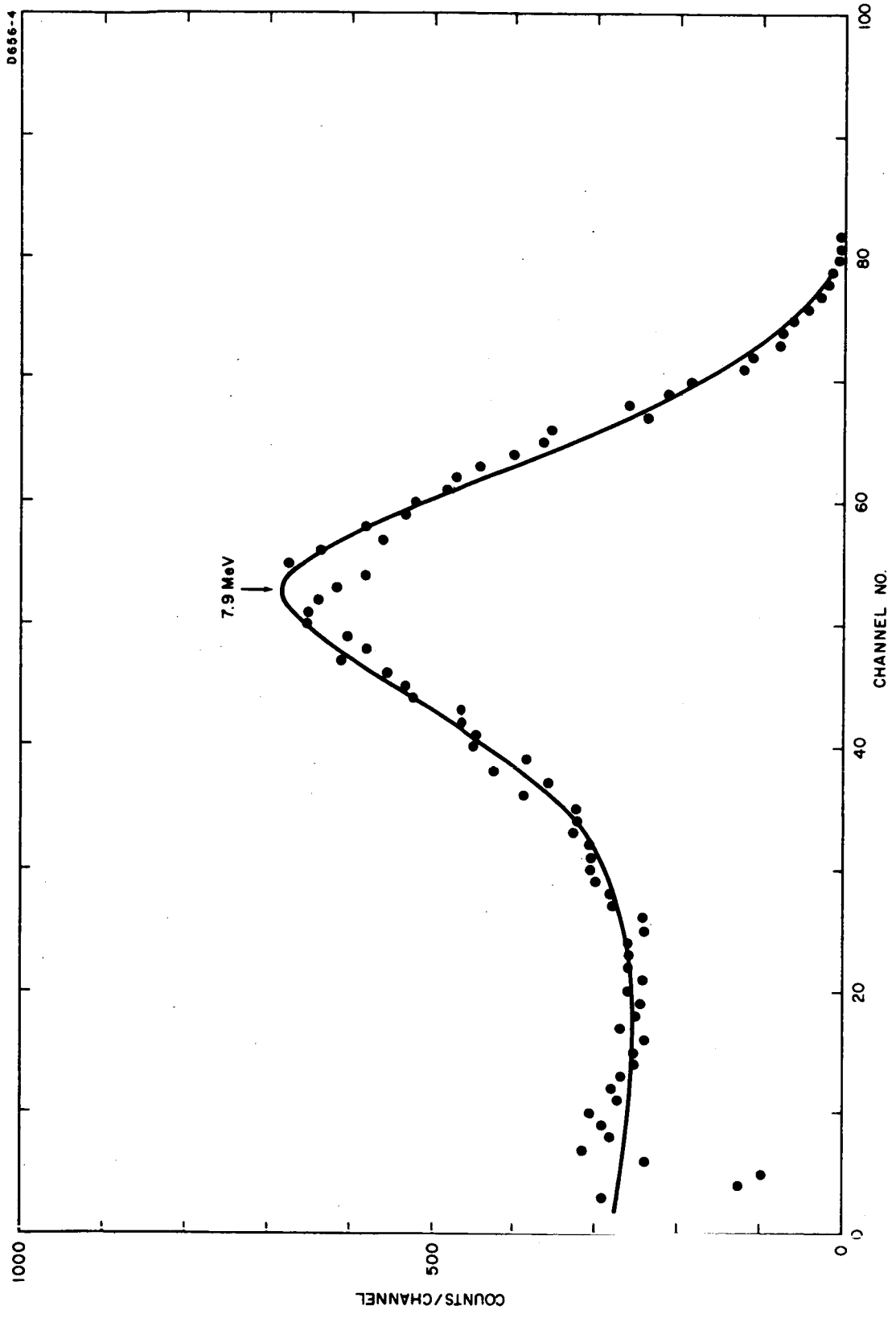

Fig. 12. Energy spectrum of 44 MeV monoenergetic protons after passage through $\simeq 1.59$ g/cm^2 of tissue-equivalent plastic.

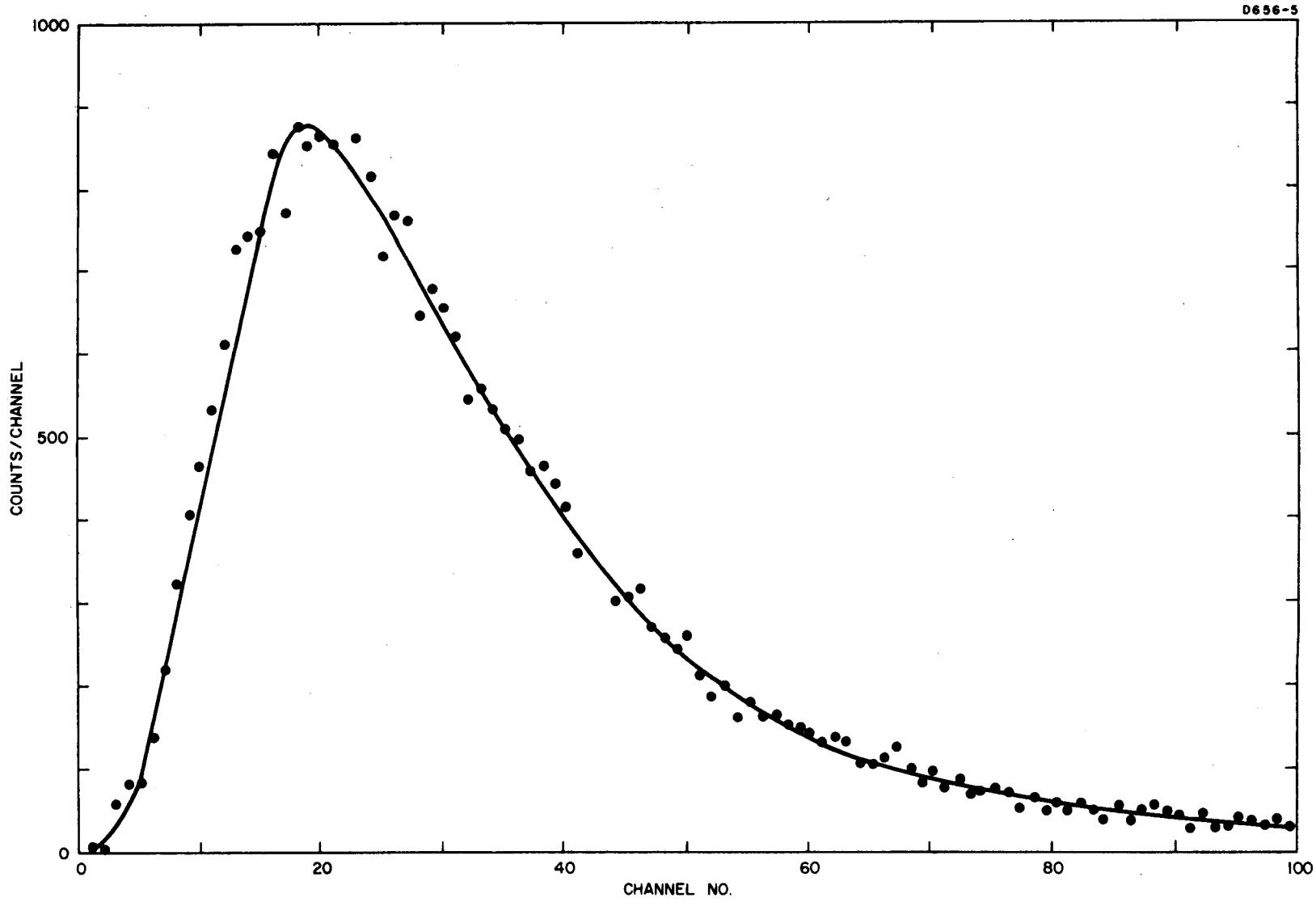

Fig. 13. Energy deposition spectrum in simulated 1.18 microns of tissue due to protons with an initial energy of 44 MeV, after passage through 0.21 g/cm^2 of tissue-equivalent plastic.

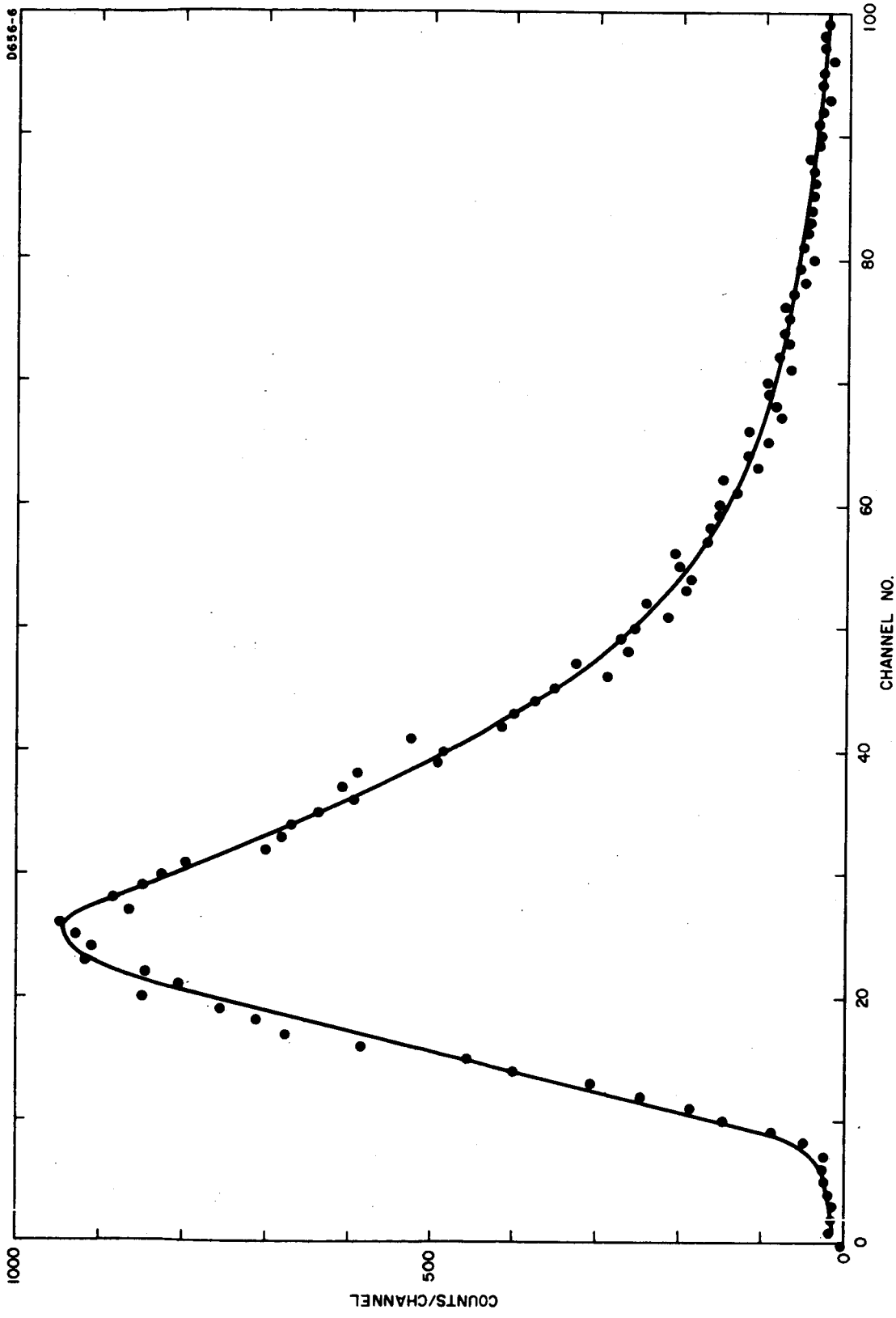

Fig. 14. Energy deposition spectrum in simulated 1.18 microns of tissue due to protons with an initial energy of 44 MeV, after passage through 1.35 g/cm^2 of tissue-equivalent plastic.

Unfortunately, differences between coincidence spectra and collimated only spectra were evidenced, resulting, in the worst case, in a shift in the peak of the distribution from channel 42 for the coincidence spectrum to channel 50 for the collimated only spectrum. This is believed to be due primarily to a poor geometrical situation, resulting in a divergent lower energy component scattering from the collimator. Evidence for this is also seen in the p-i-n energy spectra obtained. These show a significant number of particles leaving less energy than those passing through the entire detector length. Because of these factors the non-coincidence spectra should be considered to show general trends only. Additional experiments to explore the actual irradiation conditions would be necessary before more definitive data could be obtained in this manner with this beam. The coincidence spectra, selecting only peak energy protons entering the detector essentially parallel to the nominal beam direction, should, of course, still be valid.

The pertinent results of the non-coincidence spectra are presented in Fig. 15 and table IV. In Fig. 15 the distributions at different depths have been normalized to the same number of counts in the peak channel and to the same peak channel, to more clearly show the manner in which the distributions are changing with depth. The trends seen in table IV will be noted to agree with those for the lower energy shown in table III, and the same explanatory comments are therefore pertinent in this case. Of particular interest in this case are the last three depths examined. These correspond to the "Bragg peak" (11.05 g/cm^2) and points at 67% of the peak (11.41 g/cm^2) and 39% of the peak (11.61 g/cm^2), both on the rapidly falling far side of the "Bragg-type" ionization curve. The coincidence spectra for depths of 0.21 g/cm^2, 5.31 g/cm^2, and 9.56 g/cm^2 H_2O are shown in Figs. 16, 17, and 18, respectively. The system gain is the same for these three figures. None of the results obtained at this energy have thus far been corrected for noise and resolution broadening.

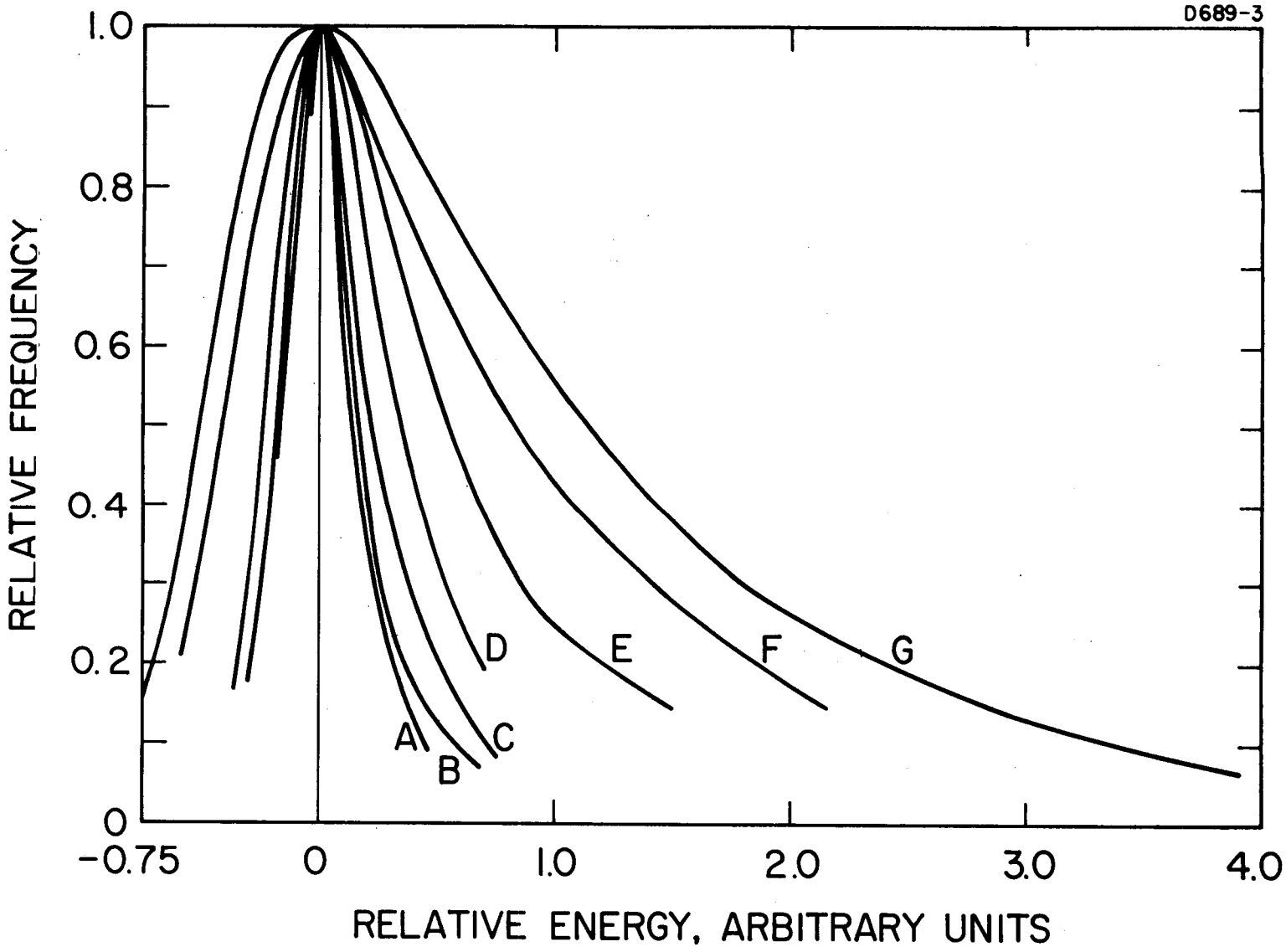

Fig. 15. Normalized energy deposition spectra in simulated 1.18 microns of tissue due to protons with an initial energy of 125.5 ± 0.8 MeV after penetration to various depths in water: A = 0.21 g/cm^2 H_2O; B = 5.31 g/cm^2; C = 9.56 g/cm^2; D = 10.56 g/cm^2; E = 11.05 g/cm^2 (Bragg peak); F = 11.41 g/cm^2; G = 11.71 g/cm^2.

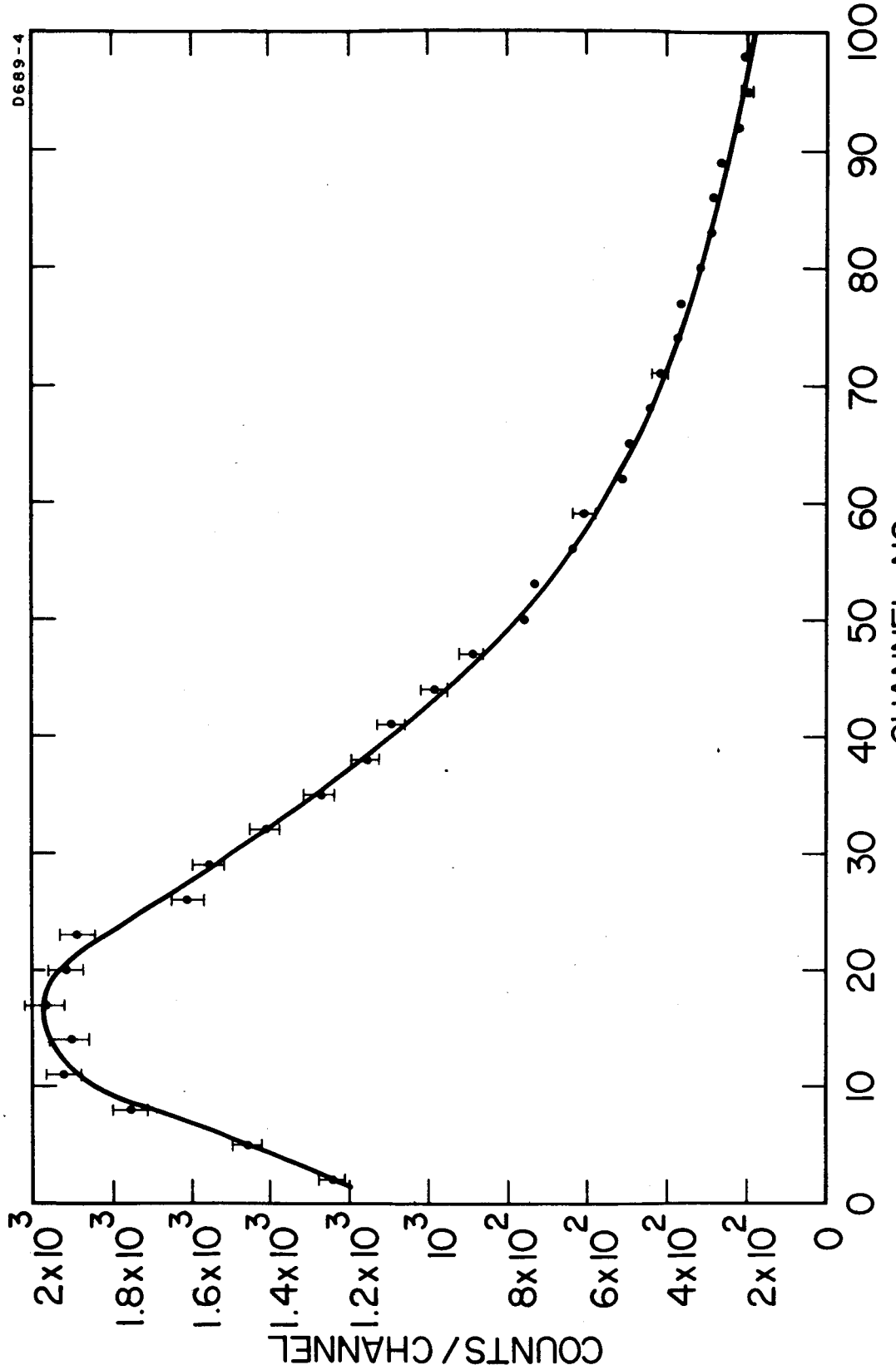

Fig. 16. Frequency distribution of energy deposition in simulated 1.18 microns of tissue due to protons with an initial energy of 125.5 ± 0.8 MeV, after penetration of 0.21 g/cm^2 H_2O.

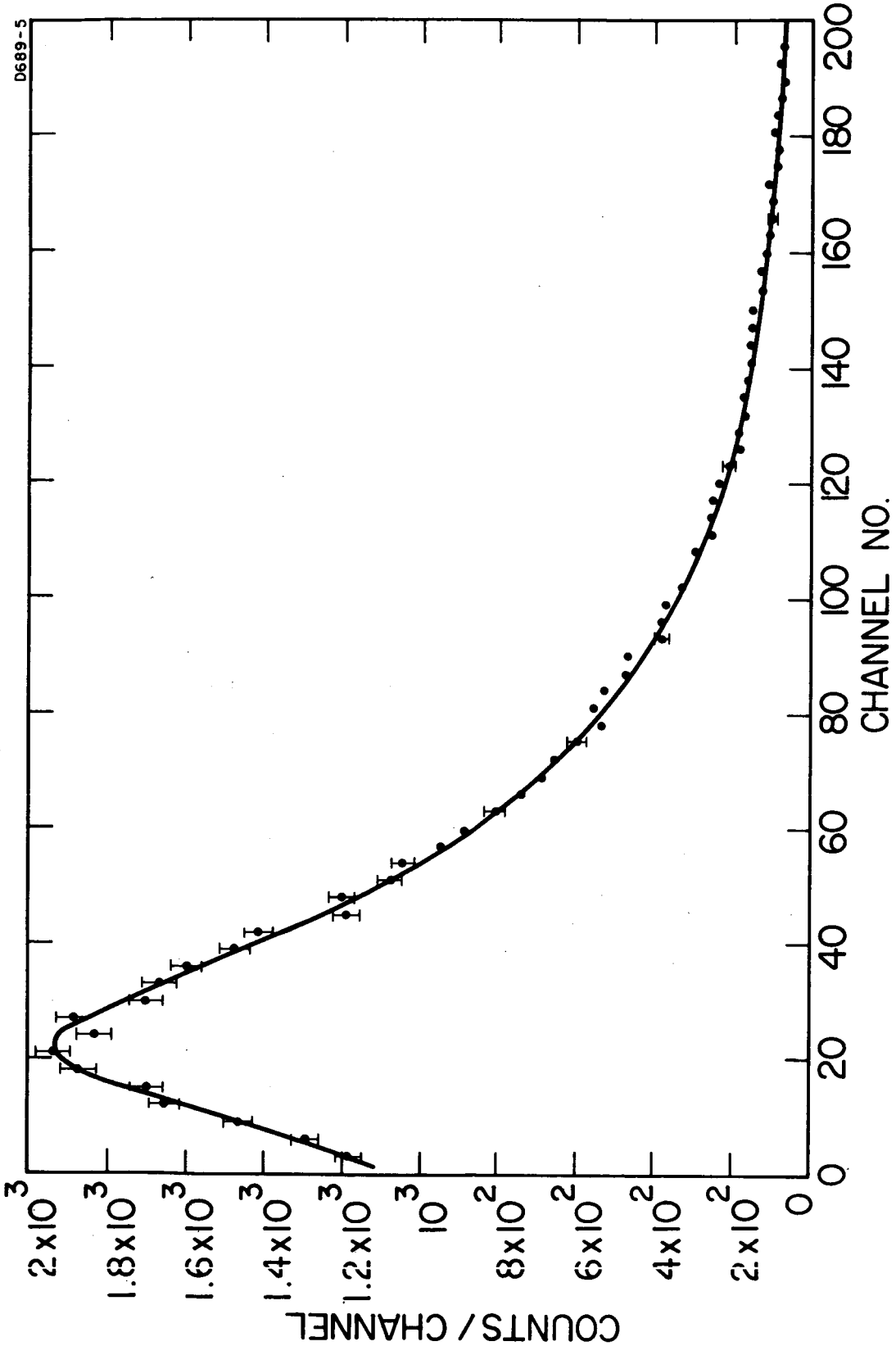

Fig. 17. Frequency distribution of energy deposition in simulated 1.18 microns of tissue due to protons with an initial energy of 125.5 ± 0.8 MeV, after penetration of 5.31 g/cm^2 H_2O.

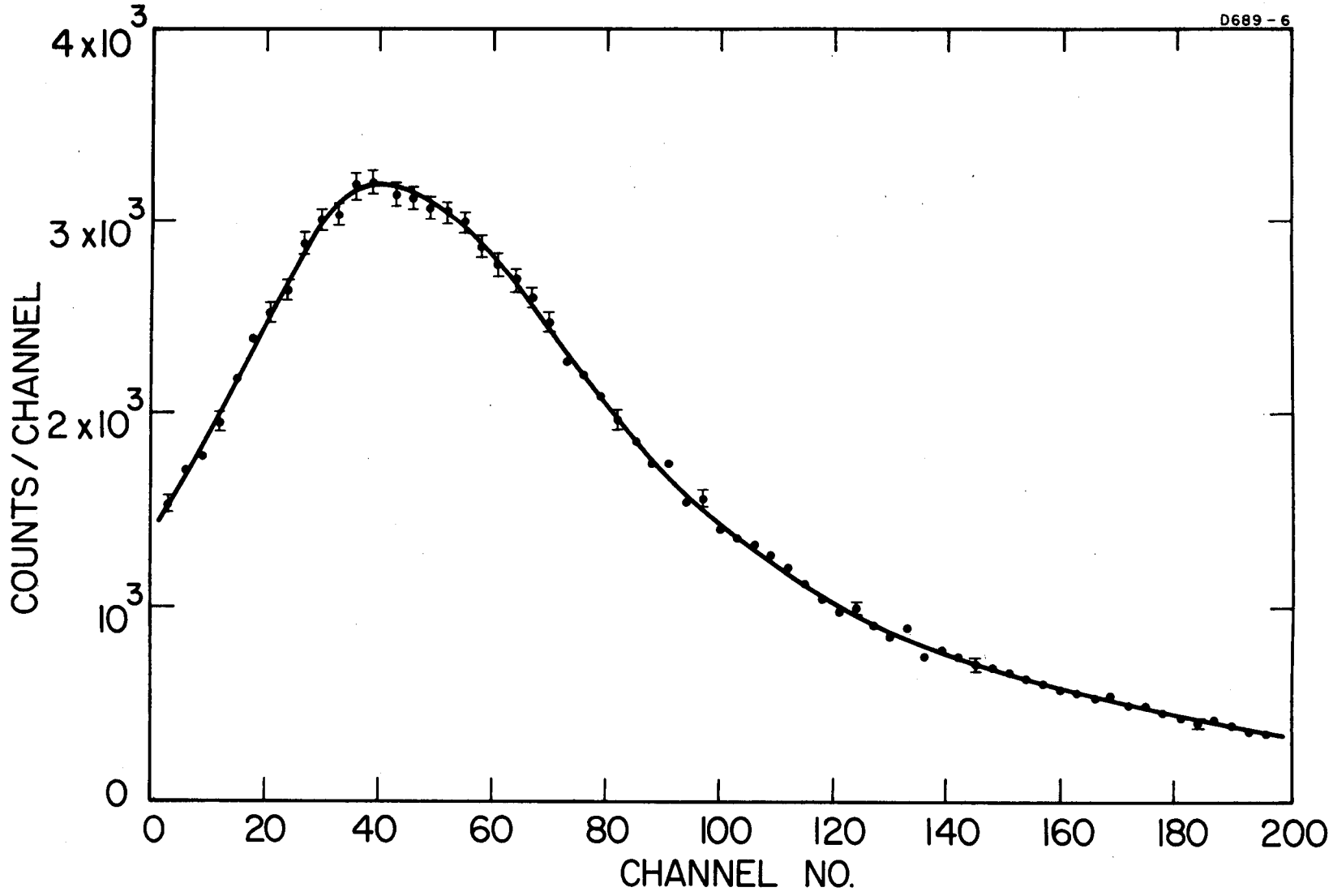

Fig. 18. Frequency distribution of energy deposition in simulated 1.18 microns of tissue due to protons with an initial energy of 125.5 ± 0.8 MeV, after penetration of 9.56 g/cm^2 H_2O.

IV. SPHERICAL SILICON Au-i-Al DETECTORS

During the past year studies were initiated to improve the quality of the silicon lithium compensated 4π detectors. These studies included, (a) methods for establishing the gold surface barrier, (b) characteristics of the aluminum contact, (c) studies of the collection efficiency as a function of the section of the sphere through which the particle enters. In these studies it was found that the current through the device was primarily a function of the processing involved with the formation of the surface barrier under the evaporated gold volume. A number of interesting aspects were discovered. One was the degree of washing required to completely free the silicon surface of the etching compounds. Barriers established on incompletely rinsed surfaces produced extremely high current devices. The quality of the barrier established was also found to be controlled quite critically by the quality of the gold evaporation. The lowest current devices were made by ultrasonically bonding a 1 mil gold wire to the device after the gold evaporation. Leads placed directly on the silicon before evaporation produced extremely high currents. It was also found that these barriers require a certain aging in a rather high humidity atmosphere. Aging of the compensated material in this same atmosphere before gold evaporation does not produce the same quality barrier as that obtained by aging after gold evaporation. With respect to the second contact, it was found that in order to get a nonrectifying ohmic contact it was necessary to evaporate the aluminum only on a lapped surface. A study of the noise characteristics as a function of the material used on this back contact is now in progress. Materials which are now being studied for back contact use are aluminum, copper, and platinum. Associated noise with each will be studied as a function of silicon surface preparation. Through the use of a collimated Sn^{113} source the collection efficiency as a function of the entrance surface has been studied. Curves of pulse height versus field strength for the various entrance positions are being obtained for each type of contact. It is hoped that these studies will yield a consistent method for obtaining low noise and complete collection efficiency for the entire bulk. The use of platinum was found to produce a better barrier on the compensated silicon than does gold. The latest spheres have been fabricated in this manner. It only remains to establish good n^+ contact.

V. CONCLUSIONS AND RECOMMENDATIONS

All the necessary groundwork has now been laid for determination of meaningful proton energy deposition spectra. The proper instrumentation has been perfected and thoroughly tested, the pertinent proton interaction parameters have been examined in detail, and preliminary exploratory runs have been completed at two energies. It has been possible, in addition, to examine some facets of proton energy loss distributions for mean energy losses lower than previously reported in the literature. Good agreement has been found with the Blunck-Leisegang corrected Vavilov theory. A thorough examination of energy deposition distributions as a function of tissue depth for protons with an initial energy of 40-45 MeV will be undertaken shortly. For protons in this energy range, in which multiple coulomb scatter evidently does not significantly affect the resulting energy deposition distributions, the distributions will be obtained at a given depth by observing the spectrum for protons passing along a diameter and changing the gas pressure to change the effective pathlength in the simulated tissue microvolume. The resulting spectra can then be folded together on the basis of the relative number of pathlengths of each value in a spherical or arbitrarily shaped volume in order to simulate the response of the entire microvolume. A computer program will be necessary for this purpose. It should be kept in mind that for a situation in which multiple coulomb scatter cannot be ignored this approach cannot be used, and more elaborate experiments would have to be carefully designed to properly account for such scatter. In the experiments to be performed in this energy range, care will be taken to obtain sufficient statistics to carefully examine the characteristic high energy tail of the energy deposition distributions. This is extremely important, since the high energy tail must be assumed to be of considerable significance biologically, and it is just in this part of the distributions that, even in many simple cases, the theoretical energy loss distributions cannot be expected to predict at all realistically the actual energy deposition distributions, because of δ-ray effects.

When energy deposition distributions have been determined for various energies and various simulated tissue microvolumes, the biological implications of these distributions should be examined by performing parallel irradiations of biological matter. It is hoped that a complete understanding of the relation between microscopic absorbed energy distributions and biological effect might lead to a general model of radiation damage which would, for example, allow predictions of proton or other heavy particle induced damage based on the widely studied and well documented effects of x-rays on biological systems.

An effort will also be made to completely characterize the response to high energy protons of the tiny spherical, silicon, Au-i-Al detectors and plastic scintillating beads. In addition to being useful for studies of high energy proton energy deposition distributions occurring in anatomical situations in which the use of spherical proportional counters is impossible due to their inherently large size, they may also be used in other geometries to investigate the dose distributions at bone-tissue interfaces, etc.

Table I

Experimental Conditions for Proton Energy Loss Distributions Examined

Counter	Proton Energy	Gas Pressure	$s = \rho t$	ξ	κ	b^2	Mean Energy Loss, $\bar{\Delta}$
-	(MeV)	(Torr)	(g/cm^2)	(keV)	-	-	(keV)
Brass	43.7	600	4.00×10^{-3}	3.57	0.0375	0.89	49.5
Brass	43.7	200	1.33×10^{-3}	1.19	0.0125	2.64	16.4
T. E.	40.3	150	1.00×10^{-3}	0.955	0.0108	3.28	13.2
Brass	43.7	100	6.66×10^{-4}	0.594	0.0062	5.30	8.22
T. E.	40.3	60	4.00×10^{-4}	0.382	0.0043	8.20	5.27
Brass	43.7	20	1.33×10^{-4}	0.119	0.0012	26.3	1.64

Table II

Proton Energy Loss Distributions

Mean Energy Loss, $\overline{\Delta}$	Ratio of Most Probable to Mean Energy Loss, $\Delta mp/\overline{\Delta}$	Vavilov	Vavilov with Blunck-Leisegang Correction	Experimental
(keV)	-	(% FWHM)		
49.5	.80	37	41	42
16.4	.72	40	52	54
13.2	.70	41	55	54[a]
8.22	.67	43	63	60
5.27	.64	46	76	78[a]
1.64	.55	52	135	136

[a]Not corrected by computer for electrical noise and counter resolution.

Table III

Summary of Absorbed Energy Deposition Parameters for a 1.18 micron Tissue Path (E_o = 44 MeV)

Depth in Tissue-equivalent Plastic	Energy of Proton Entering Microvolume	Relative Peak Height	Peak Width
(g/cm^2)	(MeV)	-	(% FWHM)
0.210	41	1.0	140
0.780	30	1.4	112
1.065	25	1.8	106
1.209	22	2.1	114
1.350	18	2.6	98
1.494	14	4.0[a]	98[a]
1.636	7	8.0[a]	120[a]

[a]These energy deposition spectra were obtained using collimated beams.

Table IV

Summary of Absorbed Energy Deposition Parameters[†] for a 1.18 micron Tissue Path (E_o = 125.5 ± 0.8 MeV)

Depth in H_2O	Mean Proton Energy Entering Microvolume	Relative Peak Height	Width of Peak
(g/cm^2)	(MeV)	-	(% FWHM)
.21	124.5 ± 0.9	1.00	360
5.31	88.2 ± 1.0	1.60	275
9.56	44.4 ± 1.6	3.40	200
10.56	28.2 ± 2.5	4.94	154
11.05	16.2 ± 3.8	7.20	145
11.41	-[a]	11.6	142
11.61	-[a]	14.0	156

[†]These distributions are for a collimated beam.

[a]Mean range of 125.5 MeV protons is 11.33 g/cm^2 H_2O.

REFERENCES

1. H. H. Rossi and W. Rosenzweig, "A device for the measurement of dose as a function of specific ionization," Radiology 64, 404-411 (1955).

2. H. H. Rossi and W. Rosenzweig, "Measurement of neutron dose as a function of linear energy transfer," Rad. Res. 2, 417-425 (1955).

3. H. H. Rossi, "Specification of radiation quality," Rad. Res. 10, 522-531 (1959).

4. H. H. Rossi, M. H. Biavati, and W. Gross, "Local energy density in irradiated tissues," Rad. Res. 15, 431-439 (1961).

5. H. H. Rossi, "Spatial distribution of energy deposition by ionizing radiation," Rad. Res. 2, Supplement 290-299 (1960).

6. L. Landau, "On the energy loss of fast particles by ionization," J. Phys. U.S.S.R. 8, 201 (1944).

7. P. V. Vavilov, "Ionization losses of high-energy heavy particles," Zh. Exper. Teor. Fiz. 32, 320 (1957). Transl., JETP 5, 749 (1957).

8. O. Blunck and S. Leisegang, "Zum energieverlust schneller elektronen in dünnen schichten," Z. Physik 128, 500 (1950).

9. Mudundi R. Raju, "Heavy-particle studies with silicon detectors," UCRL-16613, University of California, Berkeley (Fall 1965).

10. John S. Bevan, "Parameters describing the microscopic distribution of radiation dose," Phys. Med. Biol. 11, #3, 405-409 (1966).

11. W. H. Barkas and M. J. Berger, "Tables of energy losses and ranges of heavy charged particles," in Studies in Penetration of Charged Particles in Matter, NAS-NRC Publ. no. 1133, 103 (1964).

12. W. Rosenzweig and H. H. Rossi, "Statistical fluctuations in the energy loss of 5.8 MeV alpha particles passing through an absorber of variable thickness," Columbia Radiological Research Laboratory Report NYO-10716, Nov. 1963 (unpublished).

13. K. R. Symon, "Fluctuations in energy loss by high energy charged particles in passing through matter," Thesis (Harvard University, 1948).

14. B. Rossi, High Energy Particles (Prentice-Hall, Inc., Englewood Cliffs, N.J., 1952), pp. 29-37.

15. J. L. Campbell and K. W. D. Ledingham, "Pulse height distributions from proportional counters," Brit. J. Appl. Phys. 17, 769-774 (1965).

16. S. Saltzer and M. Berger, "Energy-loss straggling of protons and mesons: tabulation of the Vavilov distribution," in Studies in Penetration of Charged Particles in Matter, NAS-NCR Publ. # 1133, 187 (1964).

17. U. Fano, "Penetration of protons, alpha particles, and mesons," Ann. Rev. Nucl. Sci. 13, 1 (1963). Also published in Studies in Penetration of Charged Particles in Matter, NAS-NRC Publ. #1133, Appendix A (1964).

18. Stopping Powers for Use with Cavity Ionization Chambers, NBS Handbook 79, Supt. of Documents, Wash. D. C. (1961).

19. T. J. Gooding and R. M. Eisberg, "Statistical fluctuations in energy losses of 37-MeV protons," Phys. Rev. 105, #2, 357-360 (1957).

20. R. D. Birkhoff, "The passage of Fast Electrons through Matter," in Handbuch der Physik, Vol. XXXIV (Springer-Verlag, Berlin, 1958), p. 90.

21. M. S. Freedman, T. B. Novey, F. T. Porter, and F. Wagner, Jr., "Correction for phosphor backscattering in electron scintillation spectrometry," Rev. Sci. Instr. 27, #9, 716-719 (1956).

22. H. S. Snyder, "Fluctuations for proportional counters," Phys. Rev. 72, 181 (1947).

23. T. E. Bortner and G. S. Hurst, "Energy per ion pair for 5-MeV alpha particles in helium," Phys. Rev. 93, 1236 (1954).

24. H. Breuer, "Note on electron scattering and the ionization correction," Nucl. Instr. Methods 33, 226 (1965).

25. G. C. Hanna, D. H. W. Kirkwood, and B. Pontecorvo, "High multiplication proportional counters for energy measurements," Phys. Rev. 75, 985 (1949).

26. P. Rothwell, "Fluctuations in the energy-loss of fast electrons in a proportional counter," Proc. Phys. Soc. B, 64, 911 (1951).

27. D. West, "Measurements of the energy loss distribution for minimum ionizing electrons in a proportional counter," Proc. Phys. Soc. A, 66, 306 (1953).

28. E. F. Bradley, "Energy loss distribution for minimum ionizing electrons in a pressure proportional counter," Proc. Phys. Soc. A, 68, 549 (1955).

29. S. Kageyama, K. Nishimura, and Y. Onai, "The straggling of fast electrons," J. Phys. Soc. Japan 8, 682-683 (1953).

30. J. Janni, "Calculations of Energy Loss, Range, Pathlength, Straggling, Multiple Scattering, and the Probability of Inelastic Nuclear Collisions for 0.1- to 1000-MeV Protons," Technical Report No. AFWL-TR-65-150, Air Force Weapons Laboratory (1966).